Molecular Cell

Article

# HSP70 binds to specific non-coding RNA and regulates human RNA polymerase III

## Graphical abstract

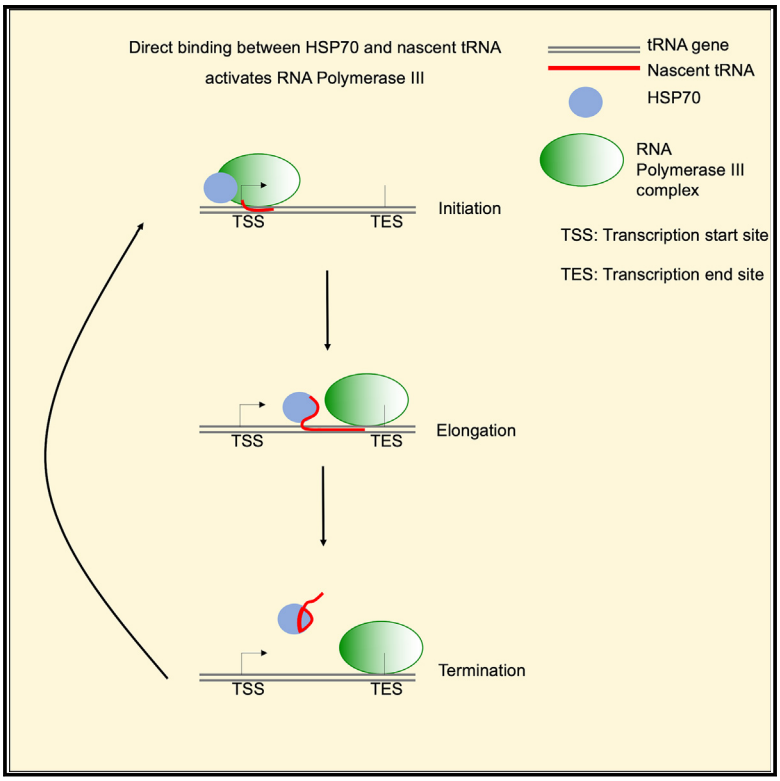


## Authors

Sergio Leone, Avinash Srivastava, Andrés Herrero-Ruiz, ..., Patrik Andersson, Anne E. Willis, Ritwick Sawarkar

## Correspondence

sergio.leone@hotmail.it (S.L.), rs2099@cam.ac.uk (R.S.)

## In brief

Leone and Srivastava et al. describe the direct interaction of chaperone proteins with RNA in human cells. They describe the localization of HSP70 on genes transcribed by RNA polymerase III. HSP70 interacts with the transcribed tRNA, and this interaction alleviates the inhibitory effect of cognate tRNA transcript on tRNA gene transcription.

## Highlights

- Chaperone proteins interact with RNA in human cells
- HSP70 binds to non-coding RNA
- HSP70 occupies RNA polymerase III-transcribed genes
- HSP70 regulates RNA polymerase III transcription

Leone et al., 2024, Molecular Cell *84*, 1–15
February 15, 2024 
https://doi.org/10.1016/j.molcel.2024.01.001

CellPress

Please cite this article in press as: Leone et al., HSP70 binds to specific non-coding RNA and regulates human RNA polymerase III, Molecular Cell (2024), https://doi.org/10.1016/j.molcel.2024.01.001

Molecular Cell

CellPress

Article

# HSP70 binds to specific non-coding RNA and regulates human RNA polymerase III

Sergio Leone,[1,4,9,*] Avinash Srivastava,[1,9] Andrés Herrero-Ruiz,[1] Barbara Hummel,[2] Lena Tittel,[2,5] Roberto Campalastri,[1] Fernando Aprile-Garcia,[2,6] Jun Hao Tan,[1,7] Prashant Rawat,[2,8] Patrik Andersson,[3] Anne E. Willis,[1] and Ritwick Sawarkar[1,2,10,*]

[1]MRC Toxicology Unit, University of Cambridge, Cambridge CB21QR, UK
[2]Max Planck Institute of Immunobiology and Epigenetics, Freiburg 79108, Germany
[3]Safety Innovation, Clinical Pharmacology and Safety Sciences, AstraZeneca R&D, Gothenburg 43183, Sweden
[4]Present address: AstraZeneca R&D, Cambridge, UK
[5]Present address: Institute of Pharmacy and Biochemistry, University of Mainz, Mainz, Germany
[6]Present address: Cytena GmbH, Freiburg, Germany
[7]Present address: Cancer Research Malaysia, Subang Jaya, Malaysia
[8]Present address: Institute of Biochemistry, ETH, Zürich, Switzerland
[9]These authors contributed equally
[10]Lead contact
*Correspondence: sergio.leone@hotmail.it (S.L.), rs2099@cam.ac.uk (R.S.)
https://doi.org/10.1016/j.molcel.2024.01.001

## SUMMARY

Molecular chaperones are critical for protein homeostasis and are implicated in several human pathologies such as neurodegeneration and cancer. While the binding of chaperones to nascent and misfolded proteins has been studied in great detail, the direct interaction between chaperones and RNA has not been systematically investigated. Here, we provide the evidence for widespread interaction between chaperones and RNA in human cells. We show that the major chaperone heat shock protein 70 (HSP70) binds to non-coding RNA transcribed by RNA polymerase III (RNA Pol III) such as tRNA and 5S rRNA. Global chromatin profiling revealed that HSP70 binds genomic sites of transcription by RNA Pol III. Detailed biochemical analyses showed that HSP70 alleviates the inhibitory effect of cognate tRNA transcript on tRNA gene transcription. Thus, our study uncovers an unexpected role of HSP70-RNA interaction in the biogenesis of a specific class of non-coding RNA with wider implications in cancer therapeutics.

## INTRODUCTION

Molecular chaperones such as heat shock proteins (HSPs) 70, 90, and small HSPs play a critical role in the folding of nascent polypeptides, stability of folded proteins, and refolding or degradation of misfolded proteins. The direct interaction of chaperones with proteins, from their synthesis to degradation, controls protein homeostasis and the functionality of the cellular proteome.[1,2] Proteotoxic stress typically leads to induction of chaperone proteins such as HSP70 and HSP90 to mitigate the proteome damage caused by stress. Age-dependent decrease in expression and malfunction of chaperones appears to be a major driver of neurodegenerative diseases.[3,4] The dependence of cancer cells on chaperone activity has led to successful pharmacological targeting of chaperones in cancer treatment.[5–7] Thus, chaperones play a pivotal role in cellular physiology, directly influencing organismal health and disease.

While the binding of chaperones to polypeptides has been extensively investigated, the direct interaction between chaperones and polynucleotides such as DNA and RNA has not been studied in detail. Chaperones are known to be implicated in several biological processes involving RNA, ranging from their biogenesis[8,9] and translation[10] to ribonucleoprotein complexes formation.[11] Interestingly, recent data suggest that RNA may itself possess chaperone activity and may further facilitate protein refolding by the prokaryotic HSP70 chaperone system.[12] A first hint of chaperone interaction with RNA was reported for the procaryotic chaperone GroEL.[13] In the context of cell extracts, HSP70 was shown to bind AU-rich sequences present at the 3′ untranslated region (3′ UTR) of several mRNA and to regulate their stability.[14–18] The interaction between HSP70 and mRNA is thought to influence mRNA stability by mechanisms that are not fully understood. It has been suggested that HSP70 recruitment to rDNA genomic loci occurs by direct binding to the newly synthetized intergenic ribosomal RNA (rRNA) in response to stresses such as heat shock or acidosis.[19,20] Furthermore, the yeast homolog of HSP70 (Ssa2p) has been described to interact with tRNA in the cytoplasm and mediate tRNA import into the nucleus under starvation conditions.[21]

Please cite this article in press as: Leone et al., HSP70 binds to specific non-coding RNA and regulates human RNA polymerase III, Molecular Cell (2024), https://doi.org/10.1016/j.molcel.2024.01.001



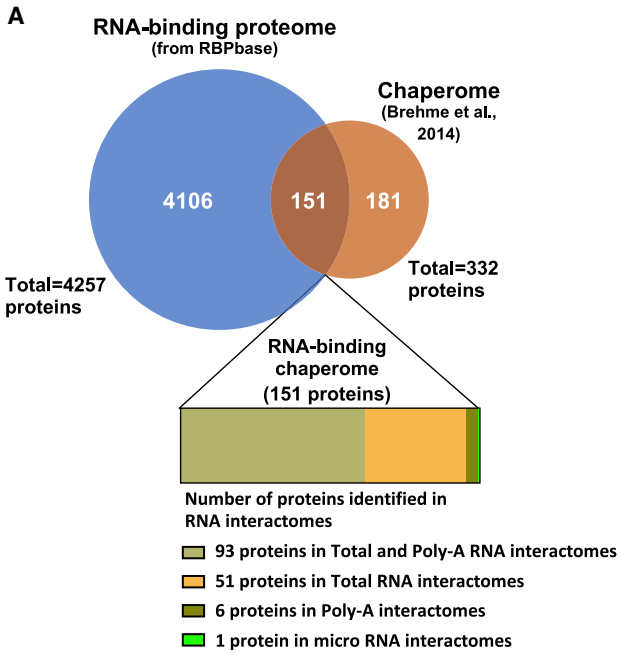


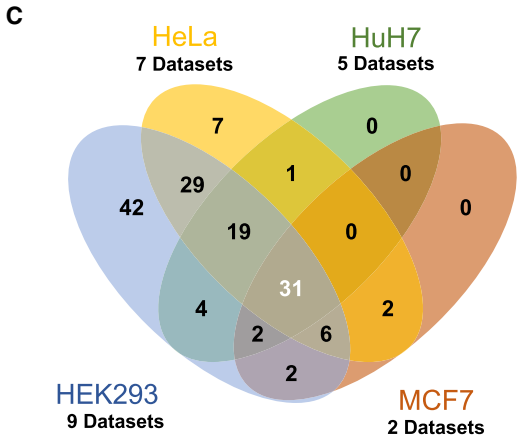


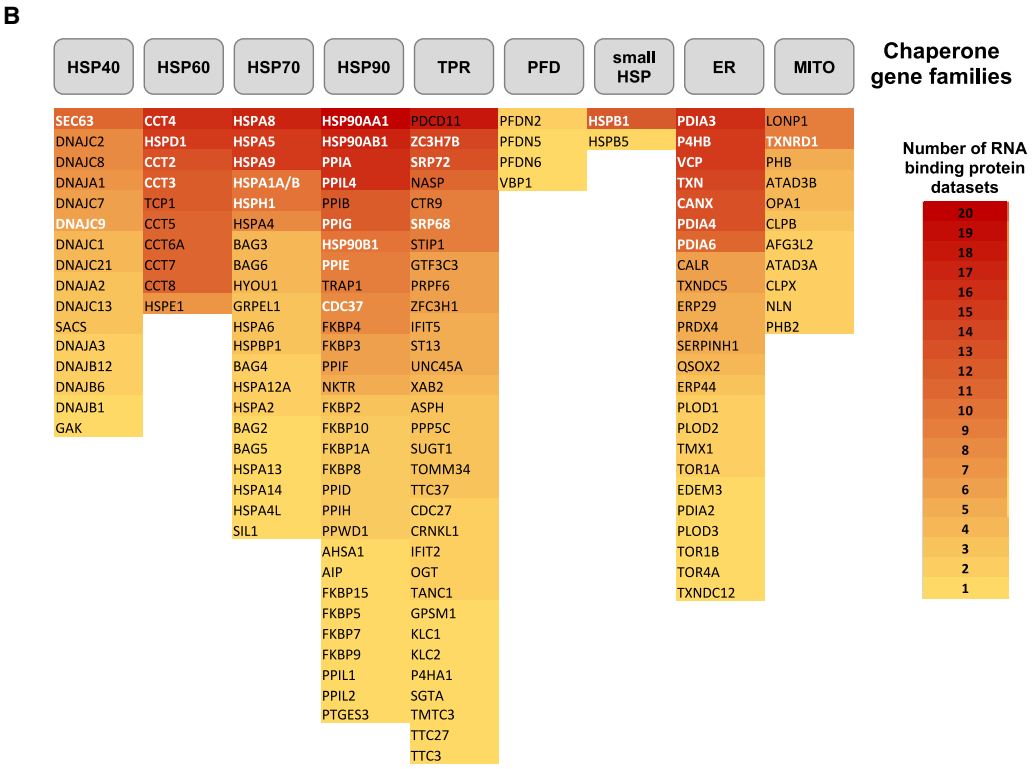


*(legend on next page)*

Please cite this article in press as: Leone et al., HSP70 binds to specific non-coding RNA and regulates human RNA polymerase III, Molecular Cell (2024), https://doi.org/10.1016/j.molcel.2024.01.001



HSP70 is an ATP-dependent chaperone consisting of an N-terminal nucleotide-binding domain (NBD) linked to a C-terminal substrate-binding domain (SBD). HSP70 chaperone activity is based on an allosteric mechanism that couples ATP hydrolysis in the NBD to substrate binding by the SBD in a cycle of association and release that prevent substrate aggregation and promote folding.[2] Both NBD and SBD can be targeted by small molecule inhibitors that reduce HSP70 activity and have been tested for cancer treatment in several clinical trials.[6] There is no known RNA-binding domain in HSP70 or any other chaperone protein, raising the question if chaperones directly bind to RNA in intact cells or if chaperone-RNA interaction is an artifact of promiscuous interactions in cell extracts.

Recent unbiased studies have identified several proteins that directly interact with RNA but do not have a canonical RNA-binding domain.[22–28] These studies make use of UV-induced crosslinks between proteins and their interacting RNA in intact cells, suggesting the possibility of non-canonical ways of RNA-protein interactions in cells. We investigated whether chaperones bind RNA in human cells, and if chaperone-RNA interaction has any functional relevance.

## RESULTS

### The RNA-binding chaperome

Recent proteome-wide studies have identified a large number of eukaryotic proteins that directly interact with RNA in cells.[25,27–29] RBPbase, a comprehensive database that integrates several independent datasets, reports 4,257 RNA-binding proteins in the human proteome (RBPbase: https://rbpbase.shiny.embl.de). To systematically investigate whether chaperones have been found in the published proteome-wide studies of RNA-binding proteins, we focused 332 proteins that constitute the human chaperome.[3] 151 chaperome proteins were reported as RNA-binding proteins (Figure 1A; Table S1). 93 out of these 151 proteins were found in the interactome of poly(A) RNA (Figure 1A), implicating around one third of the chaperome in direct interaction with mRNA. At least one member of each chaperome family was identified as an RNA-binding protein, with 33 chaperome proteins detected in more than 10 independent datasets (Figure 1B; Table S1). There was a large overlap among several distinct studies generated using four human cell lines, with 31 chaperome proteins identified in all 23 datasets (Figure 1C; Table S2). We focused on HEK293 as data from this cell line reported the largest number of RNA-binding chaperome proteins (Figures 1C and S1A). There was little correlation between expression levels of chaperome proteins and their detection as RNA-binding proteins in HEK293 (Figures S1B and S1C; Table S3). This observation rules out the possibility that highly expressed chaperones were likely contaminants in mass-spectrometry-based detection of RNA-binding proteins. Thus, unbiased proteome-wide studies suggest that about half of the chaperome proteins directly bind to RNA in human cells.

To experimentally validate the proteome-wide studies, we expressed selected chaperome proteins with C-terminal FLAG-hexa-histidine-biotin (3FHBH) tag[30,31] in HEK293 T-Rex cells. UV-crosslinking was used in intact cells to covalently link chaperones with their interacting RNA. Tandem affinity purification of the chaperome proteins using hexa-histidine and biotin tags with stringent washes allowed us to enrich protein-RNA complexes. We visualized chaperome proteins in an autoradiograph after radiolabeling the crosslinked RNA using $^{32}$P-ATP and polynucleotide kinase (PNK; Figure 2A). RNase-I-sensitive radioactive signal above and at the size of the tagged chaperome protein represented covalent protein-RNA complex, as seen for all tested chaperome proteins (Figures 2B–2E) except for small HSPs (Figure 2D). RNA-binding proteins such as HNRNPC and GAPDH[32] served as positive controls for PNK assay (Figure 2F). Thus, our experiments provide direct evidence that several chaperome proteins directly bind to RNA, raising the question about the role of chaperones in RNA synthesis, stability, and/or function.

### HSPA1A binds to RNA in cells and *in vitro*

To identify the significance of chaperone-RNA interactions, we focused on HSP70 family member HSPA1A, which showed strong interaction with RNA in PNK assays (Figure 2B). HSPA1A, and its identical homolog HSPA1B, are induced during heat shock; however, the protein is present at high levels without heat shock in HEK293 T-Rex cells allowing us to dissect the role of HSPA1A/B-RNA interaction in unstressed cells. To verify the direct binding of endogenous HSPA1A to RNA we applied the orthogonal organic phase separation (OOPS) method.[27] This protocol allows the enrichment in the acidic guanidinium-thiocyanate-phenol-chloroform (AGPC) interphase of protein-RNA adducts generated by UV-mediated covalent crosslinking. We performed OOPS using HEK293 T-Rex cells exposed to 254 nm UV light. UV-crosslinking resulted in the partitioning of endogenous HuR, a well-known RNA-binding protein, as well as HSPA1A/B, in the AGPC interphase. The negative-control β-tubulin was not found in the interphase (Figure 2G). Commercially available antibodies do not distinguish between the two identical proteins

**Figure 1. The RNA-binding chaperome**

(A) A Venn diagram showing the overlap between the human chaperome (from Brehme et al.[3]) and the RNA-binding proteome (from RBPbase; https://rbpbase.shiny.embl.de/, a collection of 30 independent human RNA-binding proteins datasets). The inset below the Venn diagram shows the number of RNA-binding chaperome proteins identified in poly(A), microRNA, and total RNA interactome studies.

(B) List of the 151 RNA-binding chaperome proteins shown in (A) sorted into chaperone families (TPR, tetratricopeptide repeat-domain-containing protein; PFD, prefoldin; ER, endoplasmic reticulum specific chaperome proteins; MITO, mitochondria-specific chaperome proteins). The boxes containing the protein name are color coded and sorted in descending order based on the number of independent datasets in which they were identified as RNA-binding proteins. The 31 chaperome proteins common to the four cell lines shown in (C) are written in white font. Number of datasets reporting HSPA1A and HSPA1B are merged since the two proteins have 100% amino acid identity and are not distinguishable by mass spectrometry analyses.

(C) A Venn diagram showing the overlap between RNA-binding chaperone proteins independently identified in distinct human cell lines. The number of datasets analyzed per cell line is indicated.

See also Figure S1 and Tables S1, S2, and S3.

Please cite this article in press as: Leone et al., HSP70 binds to specific non-coding RNA and regulates human RNA polymerase III, Molecular Cell (2024), https://doi.org/10.1016/j.molcel.2024.01.001



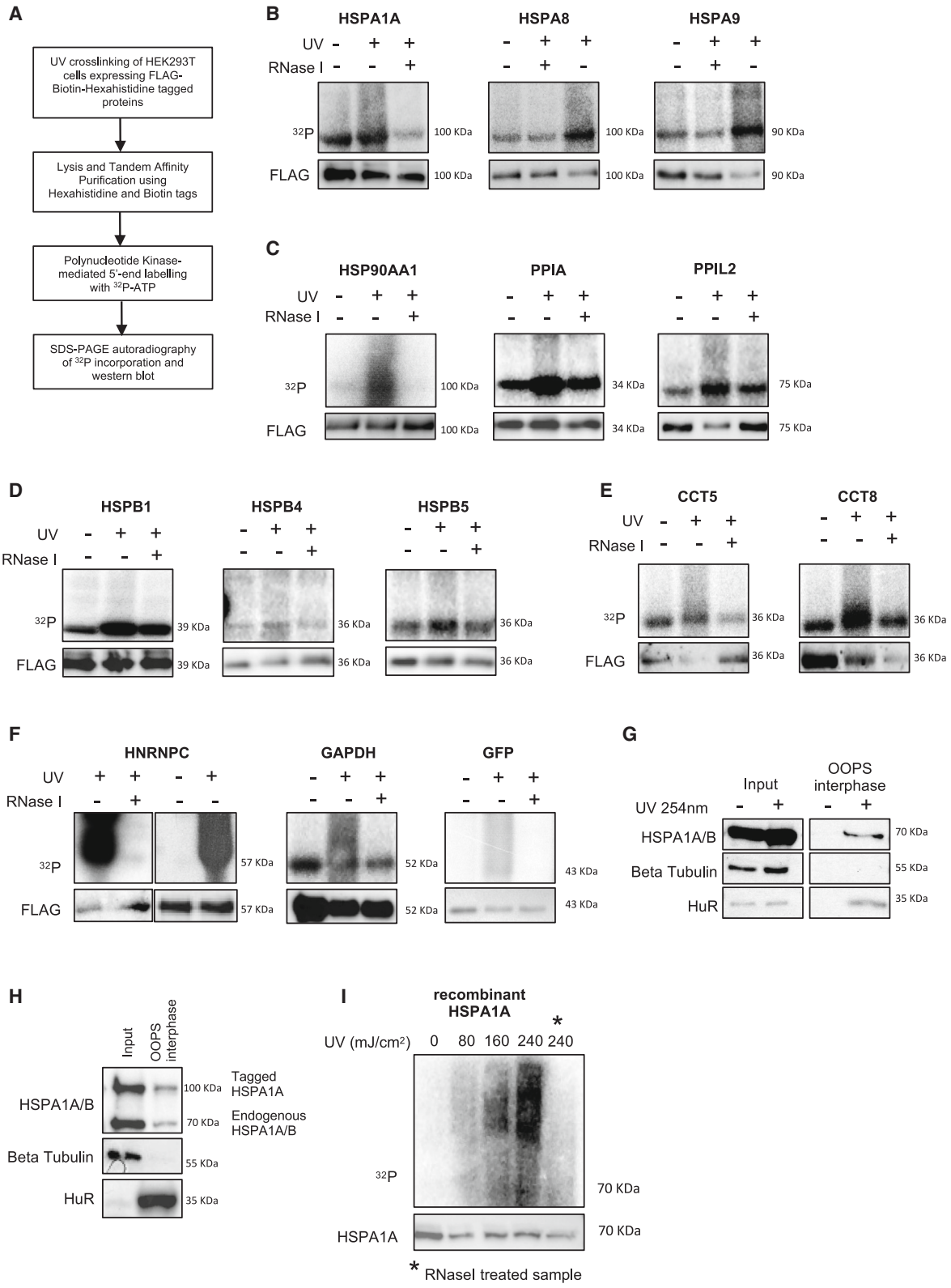


*(legend on next page)*

Please cite this article in press as: Leone et al., HSP70 binds to specific non-coding RNA and regulates human RNA polymerase III, Molecular Cell (2024), https://doi.org/10.1016/j.molcel.2024.01.001



HSPA1A and HSPA1B. Hence, we resorted to an ectopic expression of 3FHBH tagged HSPA1A. We found endogenous HSPA1A/B as well as tagged HSPA1A to partition in the AGPC interphase (Figure 2H), implying the formation of UV-crosslinked HSPA1A-RNA adducts and confirming the binding ability of HSPA1A to RNA in intact cells. To investigate whether HSPA1A can directly bind to RNA outside the cellular context, we performed *in vitro* PNK assay by UV-crosslinking recombinant HSPA1A with total RNA purified from HEK293 T-Rex cells. The *in vitro* approach confirmed the RNA-binding ability of HSPA1A as shown by the accumulation of radioactive signal that was proportional to the amount of UV radiation and sensitive to RNase I (Figure 2I). In summary, using three independent assays and conditions, our data confirm the ability of HSPA1A to directly bind to RNA in human cells.

## HSPA1A and HSPA8 bind to ncRNA

To identify the RNA species bound by HSPA1A and HSPA8 in human cells, we took advantage of the recently developed method called fast ligation of RNA after some sort of affinity purification for high-throughput sequencing (FLASH-seq; Figure 3A).[30] UV-crosslinked protein-RNA complexes were enriched by tandem affinity purification of HSPA1A or GFP as a negative control. Deep sequencing of libraries made from enriched RNA showed higher number of reads from HSPA1A/A8 compared with GFP (Figure 3B). We used Yodel peak-calling algorithm[33] to analyze HSPA1A FLASH-seq data and identified 1,087 binding sites of HSPA1A across the human transcriptome (Figures S2A and S2B; Table S4). 300 of these RNA-binding sites mapped to 28S, 5.8S, and 18S rRNA, likely reflecting the interaction of HSPA1A with the ribosome-associated chaperone complex.[34] However, upon close inspection, we found that the negative-control GFP had similar RNA-binding profile as HSPA1A/A8 on 28S, 5.8S, and 18S rRNA suggesting a non-specific binding of these rRNA to tagged proteins or to beads during purification (Figure S2C). Of the remaining 787 binding sites specifically bound by HSPA1A, around 200 mapped to simple repeats of RNA, mainly poly(A) or poly(T) (Figure S2B). This may represent HSPA1A binding to poly(A) tail of mRNA or certain repetitive RNA classes that have poly(A) and poly(T) stretches. However, due to the low complexity of these sequences, it is difficult to attribute the binding of HSPA1A to mRNA or specific simple repeat-containing RNA.

Majority of remaining RNA-binding sites of HSPA1A mapped to non-coding RNA (ncRNA) including small nuclear RNA (snRNA), tRNA, 5S rRNA, and 7SK RNA (Figure S2A). A direct visualization of FLASH-seq reads on genome browser confirmed that HSPA1A/A8 binding was highly enriched as compared with GFP on these RNA species (Figures 3C and S2D–S2G). However, the binding of HSPA1A/A8 was specific to a subset of ncRNA, since abundantly expressed long ncRNA such as XIST, NEAT1, and MALAT1 were not bound (Figure S2D). Furthermore, HSPA1A/A8 did not bind to mRNA such as GAPDH (Figure 3D), despite its high expression as measured by precision run-on sequencing (PRO-seq) in HEK293 T-Rex cells.[35] We also did not find any binding of HSPA1A to previously reported AU-rich elements in the 3′ UTR of VEGFA gene[15] (Figure 3E) or other genes encoding oncoproteins and inflammatory mediators (Figure S2H).[14,15,17] We validated FLASH-seq data by electrophoretic mobility shift assay (EMSA) using recombinant HSPA1A and *in-vitro*-transcribed and purified tRNA-Asp-GTC-2-10. HSPA1A-tRNA complex showed a higher-molecular-weight smear in the gel (Figure 3F). Thus, we have mapped the complete repertoire of RNA directly bound by a chaperone for the first time, allowing us to address the functional relevance of the widespread chaperone-RNA interactions using HSPA1A/A8 as exemplars.

## HSPA1A is not involved in the maturation of tRNA precursors

One of the major classes of RNA bound by HSPA1A in our FLASH-seq experiment was tRNA (Figures 3C, S2A, and S2E; Table S4). The binding of HSPA1A to the ncRNA RPPH1 in addition to tRNA (Figure S3A) suggested the involvement of HSPA1A in tRNA processing driven by RPPH1. The non-coding RPPH1 RNA is the catalytic component of the RNase P ribonucleoprotein complex. RNase P is responsible for the maturation of precursor tRNAs (pre-tRNAs) by the endonucleolytic cleavage of the 5′ leader sequence of pre-tRNAs (Figure S3B).[36] We observed that HSPA1A/B co-immunoprecipitated with RNase P components RPP29, POP1, and RPP21 (Figure S3C), along with the RNA component RPPH1 (Figure S3A). To assess whether HSPA1A plays a role in the assembly, disassembly, or function of RNase P ribonucleoprotein complex, we used small molecule inhibitor of HSP70,[37] which targets ATPase activity of HSPA1A along with all other HSP70 paralogs expressed in cells. Inhibition of HSP70 did not affect the interaction of RNase P component RPP29 with HSPA1A/B (Figure S3C) or with RPPH1 RNA (Figure S3D). Furthermore, HSP70 inhibition did not change the interaction between three of the components of the RNase P, RPP29, RPP21, and POP1 as observed in co-immunoprecipitation experiments (Figure S3E), ruling out the

**Figure 2. HSPA1A binds to RNA in cells and *in vitro***

(A) Scheme showing the experimental workflow of polynucleotide kinase (PNK) assay used to investigate direct protein-RNA interactions.

(B–F) Validation of RNA-binding ability of chaperone proteins belonging to the HSP70 (B), HSP90 (C), small HSP, (D) and HSP60 (E) families, along with control proteins (F) using the PNK assay outlined in (A). Upper panels show SDS-PAGE autoradiograph of $^{32}$P incorporation. UV-crosslinking of cells and treatment with RNase I after PNK reaction are indicated above each lane. Lower panels show western blot of the affinity purified 3FHBH-tagged proteins detected with anti-FLAG antibody.

(G) Western blot of OOPS interphase purified proteins from HEK293 T-Rex cell extracts detected with indicated antibodies.

(H) Western blot of OOPS experiment performed using HEK293 T-Rex cells expressing 3FHBH tagged HSPA1A.

(I) PNK assay performed using recombinant purified HSPA1A incubated with purified total RNA from HEK293 T-Rex cells. SDS-PAGE autoradiograph of $^{32}$P-labeled RNA-protein complexes (upper) and western blot with anti-HSPA1A/B antibody detection (lower). The amount of UV irradiation used in the PNK assay is indicated in mJ/cm$^2$. * denotes the sample treated with RNase I after PNK reaction.

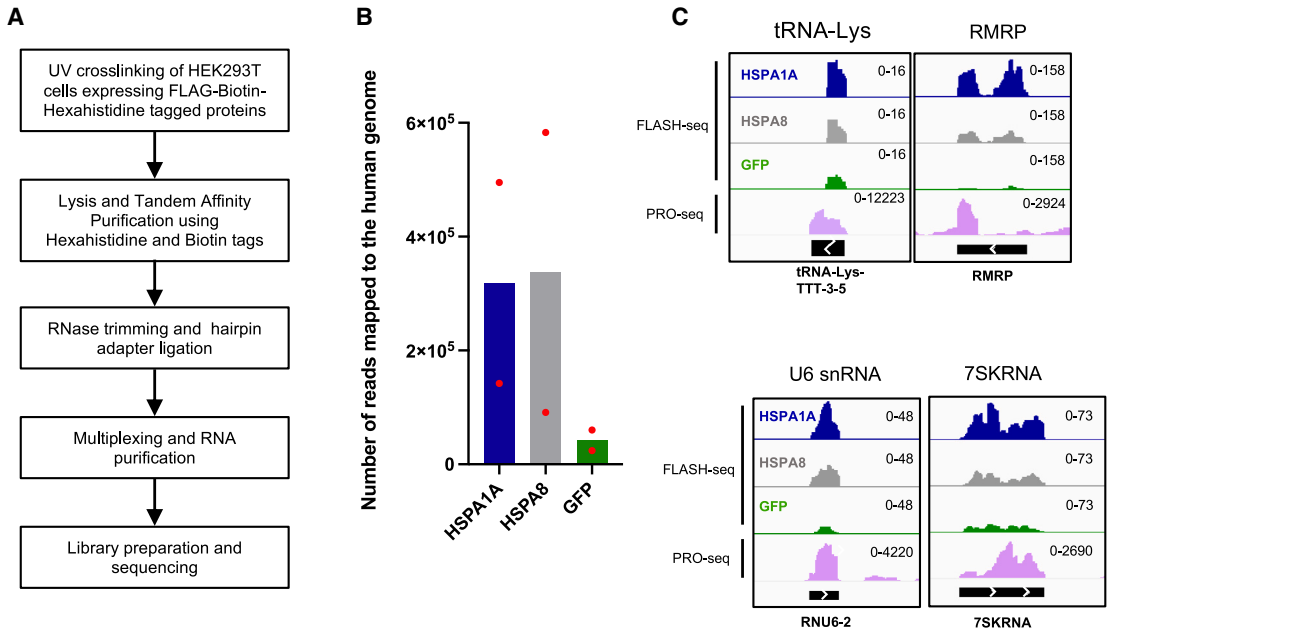


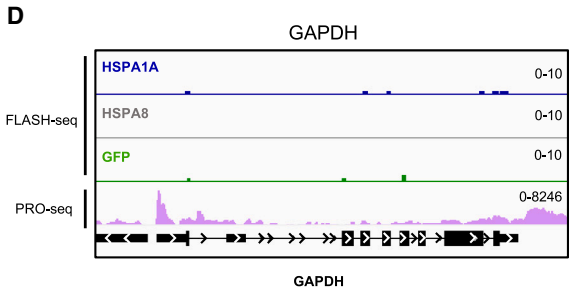


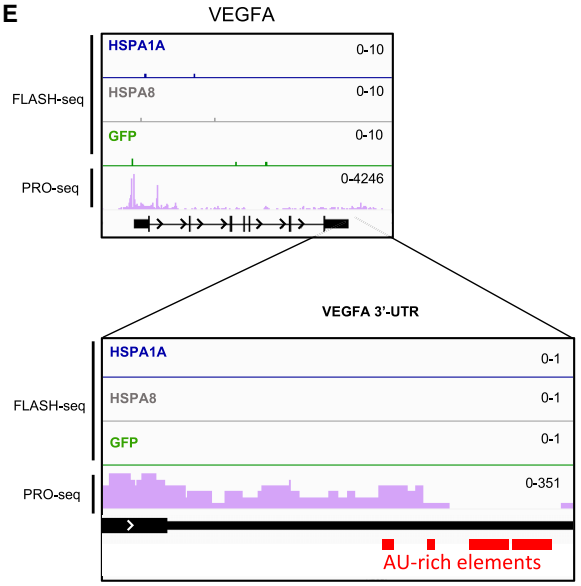


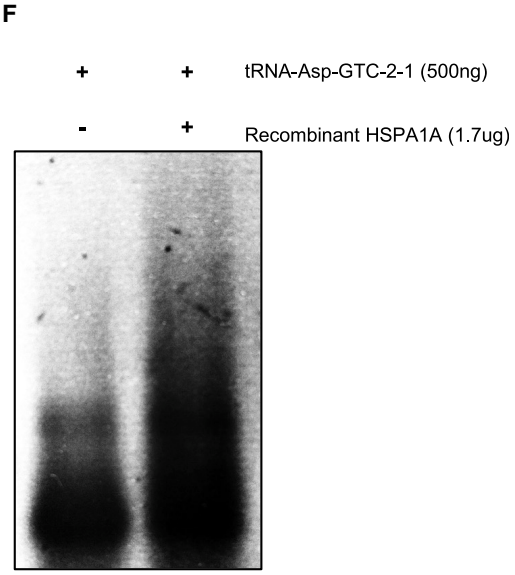


*(legend on next page)*

Please cite this article in press as: Leone et al., HSP70 binds to specific non-coding RNA and regulates human RNA polymerase III, Molecular Cell (2024), https://doi.org/10.1016/j.molcel.2024.01.001



role of HSP70 (including HSPA1A) in assembly of RNase P complex. To assess whether RNase P activity might be regulated by HSP70, we measured the efficiency of pre-tRNA processing *in vitro*, in the presence of HSP70 inhibitor or supplementing the reaction with recombinant purified HSPA1A (Figure S3F). RNase P complex was immunoprecipitated using the tagged RPP29 component. The endonucleolytic cleavage of pre-tRNA mediated by the affinity purified RNase P was comparable to the reaction catalyzed by the positive-control M1 RNA, the bacterial RNase P homolog (Figures S3G lanes 1–3 and S4C). The efficiency of pre-tRNA processing was not affected by the inhibition of HSP70 in the *in vitro* RNase P assay (Figures S3G lanes 3–4 and S4C), or by supplementing the reaction with recombinant purified HSPA1A (Figures S3H lanes 3–4 and S4D). Furthermore, HSPA1A overexpression in HEK293 T-Rex cells prior to purification of RNase P did not significantly change the activity of RNase P complex (Figures S3I lanes 3–4 and S4E). Thus, increasing the amount of HSPA1A *in vitro* or in cells did not alter RNase P activity. Altogether our data indicate that HSPA1A interacts with RNase P but does not regulate RNase P assembly or function.

## HSPA1A binds chromatin at RNA Pol III-transcribed loci

The identification of HSPA1A-bound RNA by FLASH-seq revealed an extensive binding of HSPA1A to RNA transcribed by RNA polymerase III (RNA Pol III). tRNA, RMRP, RPPH1, 7SK RNA are all products of RNA Pol III transcription (Figures 3C, S2E, and S2F). On the other hand, RNA Pol II transcripts such as mRNA and long ncRNA did not interact with HSPA1A (Figures 3D, 3E, and S2D), with the exception of snRNAs (Figure S2G). 5S rRNA—the only rRNA that is transcribed by RNA Pol III—was bound by HSPA1A (Figure S2F). The other rRNAs that are transcribed by RNA Pol I showed a non-specific binding to HSPA1A in our FLASH-seq data (Figure S2C). RNA Pol III as a common source for most RNA-interacting with HSPA1A suggested that HSPA1A may interact with RNA Pol III at chromatin and may bind RNA products co-transcriptionally. Indeed, HSPA1A/B co-affinity purified with the tagged PolR3C (Figure 4A). Similarly, the endogenous RNA Pol III component PolR3A co-affinity purified with tagged HSPA1A (Figure 4B), confirming the interaction of HSP70 with the RNA Pol III machinery in cellular extracts. To further assess whether HSPA1A could interact with RNA Pol III during transcription on genomic DNA, we mapped genome-wide binding sites of HSPA1A using chromatin immunoprecipitation followed by high-throughput sequencing (ChIP-seq). To compare the chromatin occupancy of HSPA1A with that of RNA Pol III, we identified RNA Pol III target genes which are active in HEK293 T-Rex cells as inferred from the binding of RNA Pol III.[38] Strikingly, HSPA1A occupancy around transcription start sites (TSSs) of active RNA Pol III target genes was very similar to the occupancy of RNA Pol III (Figure 4C). RNA Pol III target genes that are inactive in HEK293 T-Rex cells and did not bind to RNA Pol III, did not show any signal of HSPA1A occupancy (Figure 4D). Visualizing HSPA1A ChIP-seq and FLASH-seq reads on genome browser confirmed the chromatin co-occupancy of HSPA1A and RNA Pol III at active genes as well as the binding of the corresponding RNA to HSPA1A at majority of loci (Figures 4E, S4A, and S4B). The inactive genes were neither bound by HSPA1A nor by RNA Pol III at chromatin, and HSPA1A did not bind the corresponding ncRNA (Figure 4F).

## HSPA1A regulates RNA Pol III transcription

The co-localization of HSPA1A and RNA Pol III at chromatin (Figures 4C–4F, S4F, and S4G) and direct interaction of HSPA1A with a majority of ncRNAs transcribed by RNA Pol III (Figures 3C and S2) suggested a functional link between HSPA1A and RNA Pol III. To test the role of HSPA1A in RNA Pol III function, we performed nuclear run-on (NRO) reactions (Figure 5A) as a quantitative measure of transcriptional activity of RNA Pol III in human cells.[39] We tested a subset of RNA Pol III genes, which encoded the ncRNA bound by HSPA1A in our FLASH-seq data (Figures 3C, S2, and S3A). Inhibition of the ATPase activity of HSP70 during NRO reactions resulted in reduced transcription of RNA-Pol-III-transcribed genes compared with vehicle-treated control reactions (Figure 5B). NRO reactions use chromatin-assembled genomic DNA as template for transcription, reflecting a cellular role of HSP70 in RNA Pol III function. However, the effect of HSP70 inhibition could be indirect, for example, via the chaperone's influence on chromatin structure or nucleosomes[40] rather than the direct role of HSP70 in RNA Pol III activity. Also, HSP70 inhibitor targets all HSP70 isoforms, not just HSPA1A. We therefore employed an assay using a tRNA reporter plasmid as template for *in vitro* transcription (IVT) reactions instead of chromatin-assembled genomic DNA (Figure 5C). The reporter plasmid used in this assay contained the tRNA-Asp-GTC-2-10 gene, since both the gene locus and its transcript were bound by HSPA1A, respectively, in our ChIP-seq and FLASH-seq data (Figure S4B). Transcription of the tRNA-Asp reporter plasmid was reduced when HSP70 was inhibited in the reaction (Figure 5D). Importantly, supplementing the reaction with recombinant HSPA1A increased the transcriptional output (Figure 5E), confirming the role of HSPA1A in RNA Pol III function. The observed effect on RNA Pol III transcription was not seen when we used HSP90 inhibitor or recombinant HSP90 (Figures S5A and S5B), implying the specificity of

**Figure 3. HSPA1A and HSPA8 bind to non-coding RNAs**

(A) Scheme of FLASH-seq workflow.

(B) Number of reads mapped to the human genome obtained from FLASH-seq experiments performed using 3FHBH-tagged HSPA1A-, HSPA8-, or GFP-expressing HEK293 T-Rex cell lines. The mean of two independent replicates is shown in the bar plot along with the values for each replicate as red dots.

(C–E) Genome browser snapshots showing the distribution of HSPA1A, HSPA8, and GFP FLASH-seq reads over selected loci. Reads from precision run-on sequencing (PRO-seq) dataset show nascent transcription from the corresponding genes. The inset in (E) represents the enlarged region corresponding to the 3′ UTR of the VEGFA gene where the position of AU-rich elements is highlighted by red boxes.

(F) Electrophoretic mobility shift assay (EMSA) of tRNA-Asp-GTC-2-10 in presence or absence of recombinant HSPA1A.

See also Figures S2 and S3 and Table S4.

Please cite this article in press as: Leone et al., HSP70 binds to specific non-coding RNA and regulates human RNA polymerase III, Molecular Cell (2024), https://doi.org/10.1016/j.molcel.2024.01.001



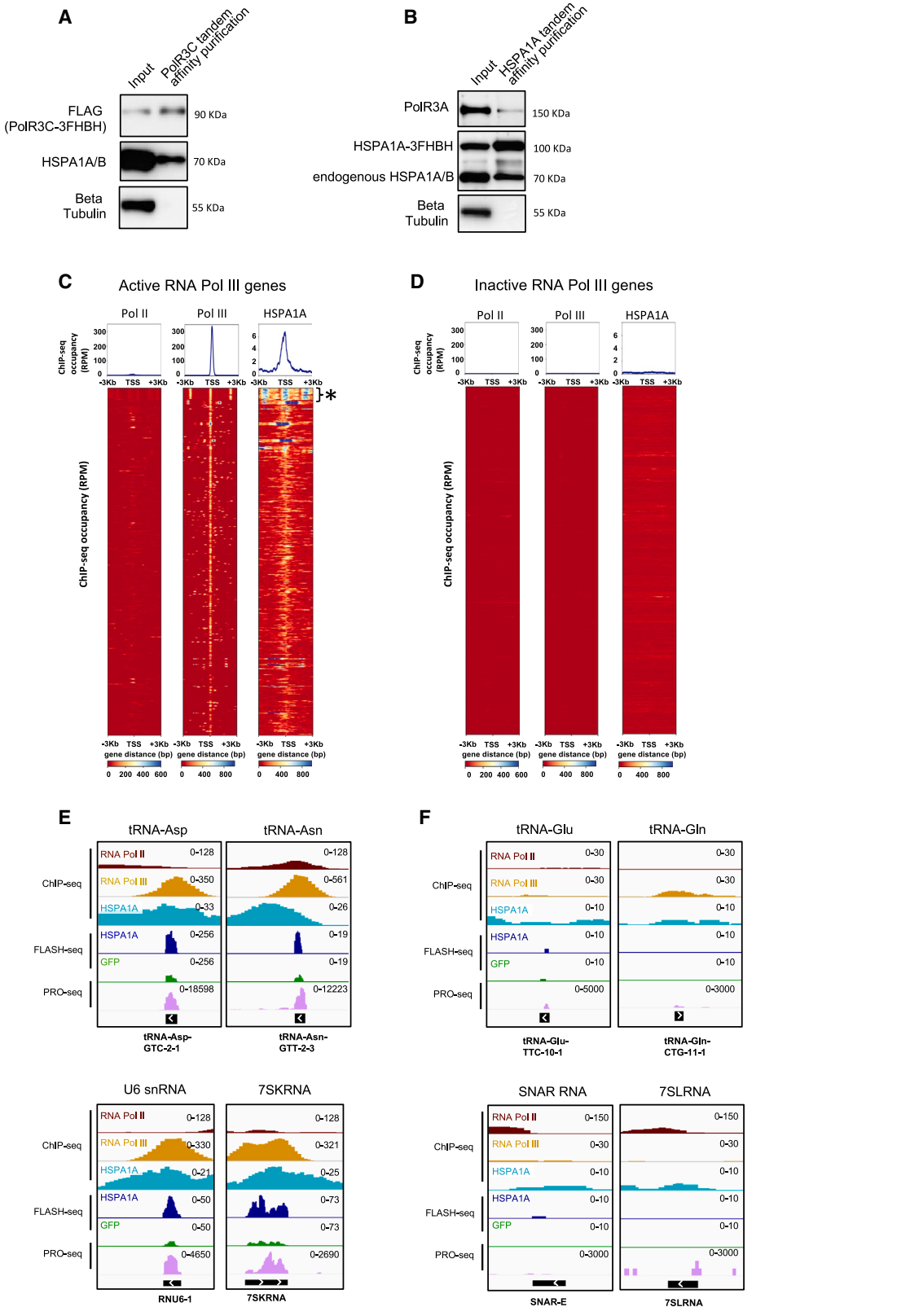


*(legend on next page)*

Please cite this article in press as: Leone et al., HSP70 binds to specific non-coding RNA and regulates human RNA polymerase III, Molecular Cell (2024), https://doi.org/10.1016/j.molcel.2024.01.001



HSP70. siRNA-mediated knockdown of HSP70 (mainly HSPA8 that could be knocked down effectively) led to downregulation of tRNA in cells and IVT assays (Figures S5C–S5E), further confirming the effects seen using the inhibitors. siRNA-mediated depletion of HSPA8 did not change levels of another ncRNA that is not bound by HSP70 according to FLASH-seq (Figure S5F), highlighting the specificity of HSPA8 function.

Total cell extracts used in the IVT reactions contain several proteins and RNA that could indirectly contribute to the effect of HSP70 inhibition on RNA Pol III transcription. Hence, we employed a refined system wherein tandem-affinity-purified RNA Pol III was used instead of total cell extracts for IVT of tRNA reporter plasmid (Figure 5F). Transcription driven by purified RNA Pol III was reduced by the presence of HSP70 inhibitor in the reaction (Figure 5G), indicating that the endogenous HSP70 copurified with RNA Pol III (Figures 4A and 4B) has an active role in modulating the transcriptional output even in a purified system. Furthermore, supplementing the reaction with recombinant HSPA1A increased the transcription of the reporter plasmid more than 4-fold compared with reaction supplemented with recombinant GFP (Figure 5H), confirming that HSPA1A acts as a positive regulator of RNA Pol III transcription.

## The mechanism of regulation of RNA Pol III by HSP70

Our experiments to understand how HSP70 enhances RNA Pol III transcription ruled out the function of HSP70 in RNA Pol III stability (Figure S6A), as may be expected from a chaperone. HSP70 did not play a role in the recruitment of RNA Pol III to its target loci either in cells (Figure S6B) or *in vitro* using plasmid templates (Figure S6C). We found no effect of HSP70 on transcription termination (Figure S6D). We then tested whether the interaction between HSP70 and RNA Pol III was RNA dependent. Surprisingly, RNase treatment during the IVT reaction caused an increased interaction between HSP70 and RNA Pol III (Figure 6A). Since this was not expected, we depleted nascent RNA from RNA Pol III in living cells using a specific inhibitor (Figure 6B), or by starvation (Figure 6C) that leads to downregulation of tRNA transcription (see Gerber et al.[41]).[42] In both cases, a decrease in nascent tRNA transcription (Figures S6E and S6F) led to an increase in interaction between HSP70 and RNA Pol III (Figures 6B and 6C), suggesting that nascent RNA from RNA Pol III inhibits the interaction between HSP70 and RNA Pol III.

To understand how RNA could influence HSP70-RNA Pol III interaction, we used mass spectrometric determination of RNA-crosslinked peptides in the tryptic digest of HSP70 after UV-crosslinking (Figure 6D).[29] A small region within the SBD of HSP70 from residue 540 to residue 550 was found to be cross-linked to and hence likely to interact with RNA. Immunoprecipitates of HSPA1A mutant lacking the region between 540 and 550 residues (d540–550) were not competent to perform IVT of tRNA gene, unlike the wild-type (WT) HSPA1A and HSPA8 (Figures 6E and S6G). The overlap between RNA-binding region and peptide-substrate-binding region within HSP70 (Figure 6D) likely explains why nascent RNA inhibits HSP70 interaction with RNA Pol III. These observations also suggested that HSP70 could regulate transcriptional activity of RNA Pol III by its interaction with nascent tRNA transcript. Exogenous addition of nascent tRNA strongly inhibited IVT of its own gene (Figure 6F) establishing a negative feedback, as shown recently.[43] Importantly, WT HSPA1A, but not d540–550 mutant, could overcome the inhibition of RNA-Pol-III-mediated transcription imposed by nascent tRNA (Figure 6G). These results suggest that HSP70 stimulates RNA Pol III activity by directly binding to nascent tRNA emerging out of RNA Pol III, overcoming the negative feedback of the nascent tRNA transcript on transcription of its own gene.

To understand whether HSP70-tRNA-RNA Pol III interaction identified in this study has any functional significance, we focused on proliferation of cancer cells, which is fueled by a steady supply of tRNA.[44] We harnessed publicly available gene expression data from The Cancer Genome Atlas (TCGA). Previous studies have reported a strong correlation in expression of genes which encode physically interacting proteins.[5] We found that the expression of several subunits of RNA Pol III is highly correlated with the expression of HSPA1A/B (Figure 6H) and HSPA8 (Figure S6H) across different cancer types from hundreds of primary tissues. Interestingly, RNA Pol III subunits, which occupy positions along the exit tunnel for nascent RNA, show strong correlation with HSPA1A/B and HSPA8 (Figure 6I), perhaps hinting at the site of interaction between HSP70 and RNA Pol III. The strong correlation between HSP70 and RNA Pol III expression in cancer transcriptomes prompted us to ask whether the two protein complexes work together to drive proliferation. While inhibiting either HSP70 or RNA Pol III on their own had reduced proliferation, a combination of the two inhibitors showed synergistic lethal effects (Figure 6J), more than expected for an additive interaction between the two inhibitors.[45] Thus, co-transcriptional interaction between HSP70, tRNA and RNA Pol III may have important functional significance in oncogenic proliferation, identifying a new potential avenue of combinatorial therapeutics.

In summary, our work provides strong evidence for the direct interaction of a large number of chaperones with RNA. Using HSP70 as an example, this study shows that the chaperone binds to specific regions of chromatin co-occupied by RNA Pol III and interacts with ncRNAs transcribed by RNA Pol III. Refined

**Figure 4. HSPA1A binds chromatin at RNA-Pol-III-transcribed loci**

(A and B) Western blot analysis of co-immunoprecipitation experiments using extracts of HEK293 T-Rex cells expressing either 3FHBH-tagged POLR3C (A) or HSPA1A (B). Co-immunoprecipitation was done by tandem affinity purification using hexa-histidine and biotin tags.

(C and D) ChIP-seq analysis of RNA Pol II, RNA Pol III, and 3FHBH-tagged HSPA1A. Metaplots (top) and heatmaps (bottom) of indicated proteins binding around transcription start sites (TSSs) of 479 active (C) and 4,105 inactive (D) RNA polymerase III-transcribed genes. y axes indicate normalized ChIP-seq occupancy in reads per million (RPM). Color-scaled intensities are in units of RPM. * indicates the 5S-rRNA gene cluster composed of 2 kb tandem repeats (see Figure S4A for a genome browser snapshot of 5S rRNA gene cluster).

(E and F) Genome browser snapshots showing RNA Pol II, RNA Pol III, and HSPA1A occupancy and the distribution of HSPA1A and GFP FLASH-seq reads over selected active (E) and inactive (F) genomic loci. Reads from precision run-on sequencing (PRO-seq) show nascent transcription from the corresponding genes. See also Figure S4.

Please cite this article in press as: Leone et al., HSP70 binds to specific non-coding RNA and regulates human RNA polymerase III, Molecular Cell (2024), https://doi.org/10.1016/j.molcel.2024.01.001



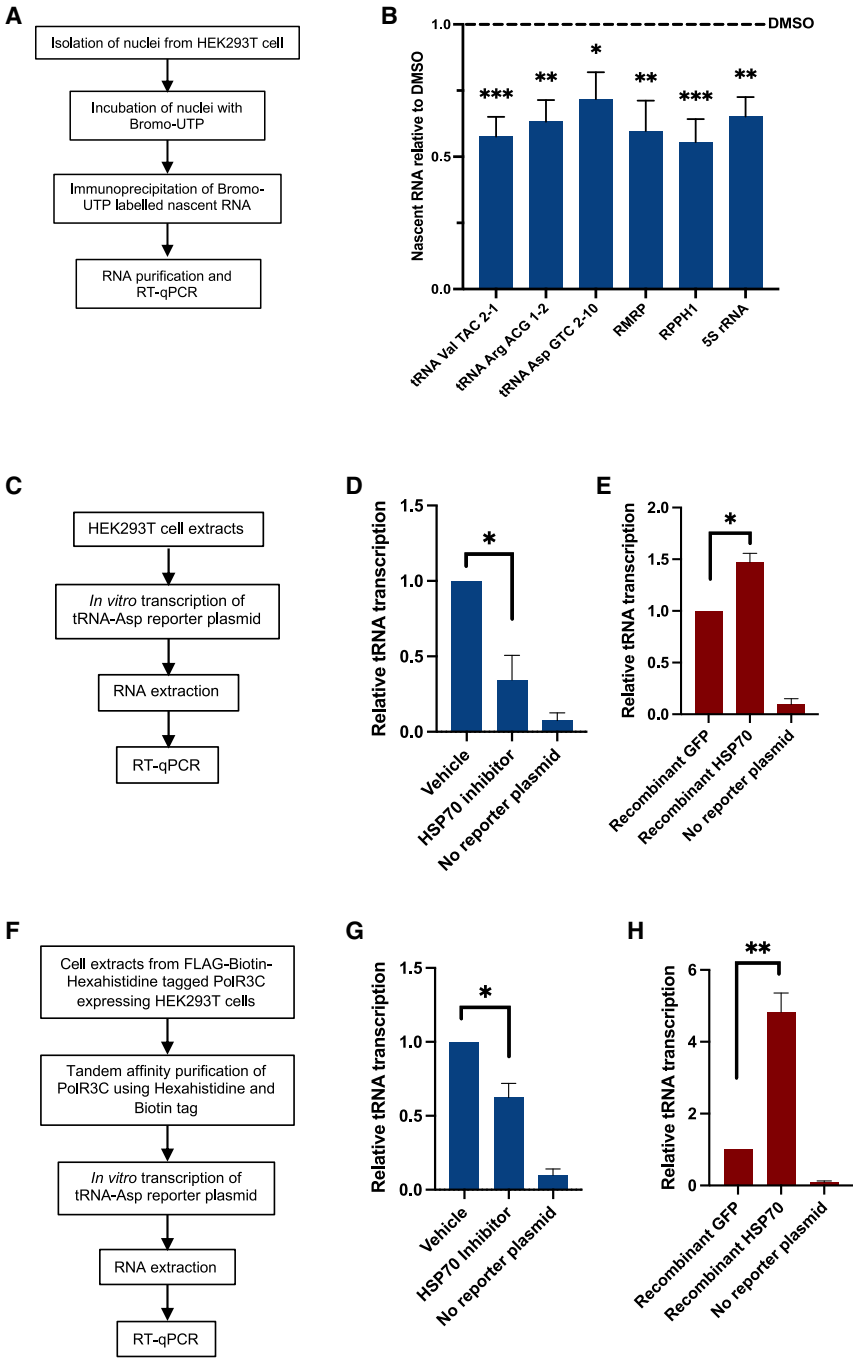


**Figure 5. HSP70 regulates RNA polymerase III transcription**

(A) Scheme of experimental workflow of nuclear run-on experiments.

(B) RT-qPCR of indicated genes after nuclear run-on experiments performed in presence of DMSO or HSP70 inhibitor. Data are normalized over vehicle control and the mean of ten replicates is shown. Error bars indicate SEM. Statistical analysis was performed using one sample t test. p value (*p = 0.05; **p = 0.01, and ***p = 0.001).

(C) Scheme of experimental workflow of *in vitro* transcription assays performed using HEK293 T-Rex cellular extracts and tRNA-Asp-GTC-2-10 reporter plasmid.

(D and E) RT-qPCR analyses of reporter tRNA transcription reaction detailed in (C). HEK293 T-Rex cellular extracts treated with HSP70 inhibitor or vehicle control (D) or supplemented with recombinant HSPA1A or recombinant GFP (E) were used in the reaction; data are normalized over vehicle control or GFP control, respectively, and the average of three (D) and four (E) independent replicates is shown. Error bars indicate SEM. Statistical analysis was performed using one sample t test. p value (*p = 0.05).

(F) Experimental workflow of *in vitro* transcription assays performed using tRNA-Asp-GTC-2-10 reporter plasmid and tandem-affinity-purified PolR3C from HEK293 T-Rex expressing 3FHBH-tagged PolR3C.

(G and H) RT-qPCR analyses of reporter tRNA transcription reaction detailed in (F). Transcription reaction performed using tandem-affinity-purified 3FHBH-tagged POLR3C. Reactions were performed in presence of HSP70 inhibitor or vehicle control (G), or recombinant HSPA1A or recombinant GFP (H). Data are normalized over vehicle or GFP control, respectively, and the mean of five (G) and four (H) independent replicates is shown. Error bars indicate SEM. Statistical analysis was performed using one sample t test. p value (*p = 0.05; **p = 0.01).

See also Figure S5.

biochemical assays suggest that HSP70 facilitates transcriptional activity of RNA Pol III by alleviating the inhibitory effect of the nascent tRNA transcript. Finally, the newly identified interaction between HSP70, RNA, and RNA Pol III could be further investigated as a potential target for cancer therapeutics.

## DISCUSSION

The unexpected widespread interaction between chaperones and RNA reported here raises two fundamental questions. First, how do chaperones contribute to RNA function, biogenesis, or stability? As highlighted in this pioneering study, the unbiased identification of chaperone-bound RNA in intact cells will likely provide clues to the breadth of chaperone function in specific aspects of RNA biology. Changes in chaperone-RNA interactions during aging and in pathological conditions will be an important area of study with ramifications on therapeutic targeting of chaperones. In this context, the role of RNA, protein-disordered domains, and molecular chaperones in biomolecular condensates formation both in healthy and diseased cells may be an exciting avenue to investigate.[46–48] The second fundamental question raised by chaperone-RNA interaction is how RNA contributes to the function of chaperones in maintaining the cellular proteome? Biochemical assays of chaperone activity carried out with

Please cite this article in press as: Leone et al., HSP70 binds to specific non-coding RNA and regulates human RNA polymerase III, Molecular Cell (2024), https://doi.org/10.1016/j.molcel.2024.01.001



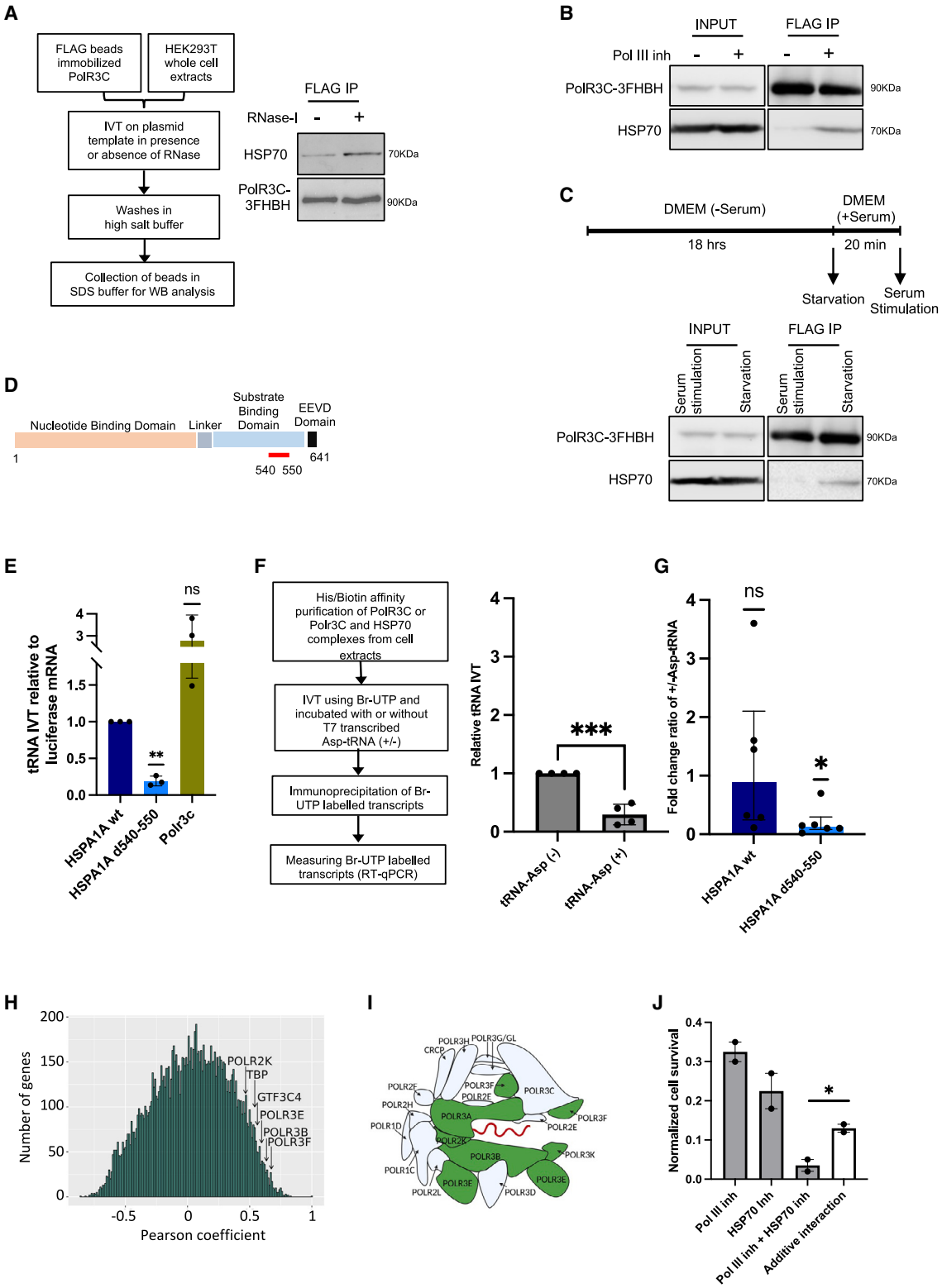


*(legend on next page)*

Please cite this article in press as: Leone et al., HSP70 binds to specific non-coding RNA and regulates human RNA polymerase III, Molecular Cell (2024), https://doi.org/10.1016/j.molcel.2024.01.001



addition of different RNA species will be key to understanding the molecular contribution of protein-RNA interactions to chaperone function. Furthermore, structural insights into chaperone-RNA interaction will be useful in identifying chaperone mutants that lack RNA-binding capacity for functional studies. The role of RNA in regulating the chaperone function during proteotoxic stress will be an important aspect to study.

Chaperones such as CCT and HSP90 are known to play a role in ribonucleoprotein assembly by directly binding protein members of the complexes.[11,49] It is likely that chaperones directly interact with RNA constituents of ribonucleoprotein complexes during the assembly process. In this regard, it is worth noting that we observed a substantial binding of HSP70 to snRNAs (Figures 3C, S2A, and S2G; Table S4), which are part of the spliceosome complex. HSP70 is shown to be a direct interactor of spliceosome components in both human and fly cells[50] and is involved in the recovery of mRNA splicing after heat inactivation.[51] Thus, the interaction of HSP70 with snRNA might be explained by a direct interaction between HSP70 and the mRNA splicing machinery in the nucleus.

The identification of endoplasmic reticulum (ER)-resident chaperones binding to RNA is surprising as the ER lumen is devoid of RNA. The ER-resident chaperones may localize briefly outside the ER lumen such as during trafficking of PDIA3 and calnexin to the cell surface in cancer cells,[52] providing an opportunity to crosslink with RNA associated with the cytosolic surface of the ER membrane.

Our inability to recapitulate HSP70 binding to intergenic rRNA and 3′ UTRs of mRNA may stem from the fact that we identified HSP70-RNA interactions that take place in intact cells, unlike previous studies that used cellular lysates to document HSP70-RNA interactions.[14,15,20] In cell lysates, RNAs can bind non-specifically to available/abundant proteins. Nonetheless, the identification of poly(A) sequences in our dataset (Figures S2A and S2B; Table S4) suggests that HSP70 may directly bind to poly(A) tails of mRNA in agreement with previous studies on HSP70-mRNA interactions. While the yeast HSP70 homolog Ssb1 has been described to directly interact with rRNA,[53] the interaction of the human HSPA1A with rRNA appears to be non-specific as our negative-control GFP also bound exactly the same sequences on rRNA (Figure S2C; Table S4). Nonetheless, HSP70 interaction with RNA reported in this study by protein-RNA crosslinking in intact cells is further corroborated by the orthogonal demonstration of chromatin binding of HSP70 precisely at the site of expression of HSP70-bound RNA (Figures 4 and S4). The interaction of HSP70 with RNA Pol III and its transcripts, and the HSPA1A occupancy of RNA-Pol-III-transcribed loci prompted us to investigate a transcriptional regulatory mechanism. Our results suggest the following model: (1) HSP70 engages with RNA Pol III machinery during initiation/elongation, (2) newly transcribed tRNA exiting the RNA Pol III machinery binds to HSP70, clearing the DNA template, (3) rapid clearance of template DNA from newly synthesized RNA allows RNA Pol III to start the next round of transcription and engage with a new HSP70 molecule.

In summary, our study provides the first global view of chaperone-RNA interaction in human cells paving an avenue to investigate how RNA and proteostasis may be functionally coupled in cells in physiology and pathology.

**Figure 6. HSP70 alleviates the inhibitory effect of nascent tRNA transcript on tRNA gene transcription**

(A) Western blot analysis of reporter tRNA transcription reaction performed using tandem-affinity-purified 3FHBH-tagged PolR3C in the presence or absence of RNase I (right). Schematic experimental workflow (left).

(B) Western blot analysis of FLAG co-immunoprecipitation performed using nuclear extracts of HEK293 T-Rex cells overexpressing PolR3C-3FHBH. Cells were either treated (+) or not treated (−) with RNA Pol III inhibitor.

(C) Experiment schematic (top). Western blot analysis of FLAG co-immunoprecipitation was performed using nuclear extracts of serum-stimulated or serum-starved cells.

(D) Schematic representation of HSPA1A protein domains. The region from amino acid position 540–550 within the substrate-binding domain is highlighted (red bar), as RNA-binding region.

(E) RT-qPCR analyses of reporter tRNA transcription reaction. Transcription reactions were performed using tandem-affinity-purified 3FHBH-tagged protein indicated. Data are normalized over HSPA1A wild-type (WT), and the mean of three independent replicates is shown. Error bars indicate SEM. Statistical analysis was performed using one sample t test. p value (**p = 0.01; ns, non-significant).

(F) Left: experimental workflow of *in vitro* transcription (IVT) assays performed using tRNA-Asp-GTC-2-10 reporter plasmid in the presence or absence of exogenous nascent tRNA-Asp-GTC-2-10 transcript. Right: RT-qPCR analysis of tRNA IVT output in presence (+) or absence (−) of exogenously added nascent tRNAAsp-GTC-2-10. qPCR primers did not amplify the exogenously added tRNA that contained variants within the primer-binding site. Transcription reactions were performed using tandem-affinity-purified 3FHBH-tagged PolR3C. The fold change transcriptional down regulation is normalized to untreated (tRNA-Asp (−)) reactions. Error bars indicate SEM. Statistical analysis was performed using the unpaired t test. p value (***p = 0.001; ns, non-significant).

(G) RT-qPCR analysis of the output of tRNA transcribed *in vitro* using tandem-affinity-purified 3FHBH-tagged PolR3C, either with wild-type or RNA-binding deletion mutant (d540–550) of HSPA1A. The fold change ratio between reactions carried out in presence (+Asp) or absence (−Asp) of tRNA-Asp-GTC-2-10 is shown. Bars indicate the median with interquartile range. Statistical analysis was performed using the Wilcoxon signed rank test. p value (*p = 0.05; ns, non-significant), compared with the expected fold change of 1 if tRNA addition did not alter the transcription reaction.

(H) Histogram showing the distribution of correlation coefficients for all human genes calculated by comparing their expression with that of HSPA1A/B in TCGA cancer RNA-seq datasets (~750 datasets from control and tumor samples). Members of RNA polymerase III complex showing highly correlated co-expression with HSPA1A/B are indicated. The cumulative probability of extracting these factors from independent draws is 2.90e−11.

(I) Scheme of RNA polymerase III complex with nascent transcript in red. The subunits whose expression in TCGA cancer datasets is highly correlated with HSPA1A/B are shown in green.

(J) Effect of RNA Pol III and HSP70 inhibitors either individually or in combination on the growth rate of acute monocytic leukemia cell line MOLM13. The mean growth rate with SEM is shown for two replicates. The white bar indicates the expected outcome of growth rates if the two inhibitors worked by additive interaction. The observed experimental outcome of the combination treatment is significantly lower than that of the expected outcome. Statistical analysis was performed using unpaired t test. p value (*p = 0.05).

See also Figure S6.

## Limitations of the study

The overlap between RNA-binding region and substrate-binding region of HSP70 has severely limited creation of "separation-of-function" mutants, i.e., a mutant that can bind RNA but not substrate, and a distinct mutant that can bind substrate but not RNA. Without such a separation of function, the study is limited in dissecting the contribution of RNA to chaperone activity of HSP70 and vice versa. Additionally, the study has not determined how HSP70 selectively binds to RNA arising out of RNA Pol III, and not the abundant mRNA or rRNA. Finally, a structural perspective of RNA-HSP70 interaction will be beneficial in providing molecular insights into mechanisms suggested by our biochemical experiments.

## STAR★METHODS

Detailed methods are provided in the online version of this paper and include the following:

- KEY RESOURCES TABLE
- RESOURCE AVAILABILITY
  - Lead contact
  - Materials availability
  - Data and code availability
- EXPERIMENTAL MODEL AND STUDY PARTICIPANT DETAILS
  - Cell culture
- METHOD DETAILS
  - Plasmid cloning
  - Plasmid transfection
  - Tandem Affinity Purification
  - Polynucleotide kinase (PNK) assay
  - Chromatin immunoprecipitation and sequencing
  - FLASH sequencing
  - Bioinformatic analysis
  - Whole cell extract preparation
  - Immunoprecipitation
  - RNase P assay
  - In vitro transcription
  - Nuclear Run-on
  - RNA purification and reverse transcription
  - RNA interference
  - RNA sequencing
  - Electrophoretic mobility shift assay (EMSA)
  - TGCA analysis

## SUPPLEMENTAL INFORMATION

Supplemental information can be found online at https://doi.org/10.1016/j.molcel.2024.01.001.

## ACKNOWLEDGMENTS

We would like to thank A. Akhtar, T. Aktas, V. Dezi, M. Elzek, V. Hilgers, I.A. Ilik, N. Jarrous, M. Pizzinga, E. Trompouki, and M. Colin for reagents, scientific discussions, and technical assistance. We also thank proteomics and deep sequencing facilities of Max Planck Institute of Immunobiology and Epigenetics, Freiburg, Germany. This work was supported by funds from the Max Planck Society (Germany), the Medical Research Council (UK), and the European Research Council (ERC) Consolidator grant (ChaperoneRegulome—819753) to R.S.

## AUTHOR CONTRIBUTIONS

S.L. and R.S. conceived the project. S.L., A.S., and R.S. designed the experiments. S.L. and A.S. conducted the experiments. L.T., F.A.-G., J.H.T., and P.R. helped with the experiments. B.H., R.C., and A.H.-R. carried out computational analyses. S.L. and R.S. wrote the manuscript with inputs from A.S., A.E.W., P.A., and A.H.-R. R.S. supervised the study.

## DECLARATION OF INTERESTS

S.L. and P.A. are employees of AstraZeneca. F.A.-G. is employee of Cytena GmbH.

Received: February 18, 2022
Revised: October 20, 2023
Accepted: January 2, 2024
Published: January 23, 2024

## REFERENCES

1. Vabulas, R.M., Raychaudhuri, S., Hayer-Hartl, M., and Hartl, F.U. (2010). Protein folding in the cytoplasm and the heat shock response. Cold Spring Harb. Perspect. Biol. *2*, a004390.
2. Rosenzweig, R., Nillegoda, N.B., Mayer, M.P., and Bukau, B. (2019). The Hsp70 chaperone network. Nat. Rev. Mol. Cell Biol. *20*, 665–680.
3. Brehme, M., Voisine, C., Rolland, T., Wachi, S., Soper, J.H., Zhu, Y., Orton, K., Villella, A., Garza, D., Vidal, M., et al. (2014). A chaperome subnetwork safeguards proteostasis in aging and neurodegenerative disease. Cell Rep. *9*, 1135–1150.
4. Gidalevitz, T., Ben-Zvi, A., Ho, K.H., Brignull, H.R., and Morimoto, R.I. (2006). Progressive disruption of cellular protein folding in models of polyglutamine diseases. Science *311*, 1471–1474.
5. Antonova, A., Hummel, B., Khavaran, A., Redhaber, D.M., Aprile-Garcia, F., Rawat, P., Gundel, K., Schneck, M., Hansen, E.C., Mitschke, J., et al. (2019). Heat-shock protein 90 controls the expression of cell-cycle genes by stabilizing metazoan-specific host-cell factor HCFC1. Cell Rep. *29*, 1645–1659.e9.
6. Shevtsov, M., Multhoff, G., Mikhaylova, E., Shibata, A., Guzhova, I., and Margulis, B. (2019). Combination of anti-cancer drugs with molecular chaperone inhibitors. Int. J. Mol. Sci. *20*, 5284.
7. Wen, W., Liu, W., Shao, Y., and Chen, L. (2014). VER-155008, a small molecule inhibitor of HSP70 with potent anti-cancer activity on lung cancer cell lines. Exp. Biol. Med. *239*, 638–645.
8. Hummel, B., Hansen, E.C., Yoveva, A., Aprile-Garcia, F., Hussong, R., and Sawarkar, R. (2017). The evolutionary capacitor HSP90 buffers the regulatory effects of mammalian endogenous retroviruses. Nat. Struct. Mol. Biol. *24*, 234–242.
9. Sawarkar, R., Sievers, C., and Paro, R. (2012). Hsp90 globally targets paused RNA polymerase to regulate gene expression in response to environmental stimuli. Cell *149*, 807–818.
10. Willmund, F., del Alamo, M., Pechmann, S., Chen, T., Albanèse, V., Dammer, E.B., Peng, J., and Frydman, J. (2013). The cotranslational function of ribosome-associated Hsp70 in eukaryotic protein homeostasis. Cell *152*, 196–209.
11. Iwasaki, S., Kobayashi, M., Yoda, M., Sakaguchi, Y., Katsuma, S., Suzuki, T., and Tomari, Y. (2010). Hsc70/Hsp90 chaperone machinery mediates ATP-dependent RISC loading of small RNA duplexes. Mol. Cell *39*, 292–299.
12. Docter, B.E., Horowitz, S., Gray, M.J., Jakob, U., and Bardwell, J.C. (2016). Do nucleic acids moonlight as molecular chaperones? Nucleic Acids Res. *44*, 4835–4845.

13. Georgellis, D., Sohlberg, B., Hartl, F.U., and von Gabain, A. (1995). Identification of GroEL as a constituent of an mRNA-protection complex in *Escherichia coli*. Mol. Microbiol. *16*, 1259–1268.

14. Henics, T., Nagy, E., Oh, H.J., Csermely, P., von Gabain, A., and Subjeck, J.R. (1999). Mammalian Hsp70 and Hsp110 proteins bind to RNA motifs involved in mRNA stability. J. Biol. Chem. *274*, 17318–17324.

15. Kishor, A., Tandukar, B., Ly, Y.V., Toth, E.A., Suarez, Y., Brewer, G., and Wilson, G.M. (2013). Hsp70 is a novel posttranscriptional regulator of gene expression that binds and stabilizes selected mRNAs containing AU-rich elements. Mol. Cell. Biol. *33*, 71–84.

16. Kishor, A., White, E.J.F., Matsangos, A.E., Yan, Z., Tandukar, B., and Wilson, G.M. (2017). Hsp70's RNA-binding and mRNA-stabilizing activities are independent of its protein chaperone functions. J. Biol. Chem. *292*, 14122–14133.

17. Wilson, G.M., Sutphen, K., Bolikal, S., Chuang, K.Y., and Brewer, G. (2001). Thermodynamics and kinetics of Hsp70 association with A + U-rich mRNA-destabilizing sequences. J. Biol. Chem. *276*, 44450–44456.

18. Zimmer, C., Von Gabain, A., and Henics, T. (2001). Analysis of sequence-specific binding of RNA to Hsp70 and its various homologs indicates the involvement of N- and C-terminal interactions. RNA *7*, 1628–1637.

19. Jacob, M.D., Audas, T.E., Uniacke, J., Trinkle-Mulcahy, L., and Lee, S. (2013). Environmental cues induce a long noncoding RNA-dependent remodeling of the nucleolus. Mol. Biol. Cell *24*, 2943–2953.

20. Audas, T.E., Jacob, M.D., and Lee, S. (2012). Immobilization of proteins in the nucleolus by ribosomal intergenic spacer noncoding RNA. Mol. Cell *45*, 147–157.

21. Takano, A., Kajita, T., Mochizuki, M., Endo, T., and Yoshihisa, T. (2015). Cytosolic Hsp70 and co-chaperones constitute a novel system for tRNA import into the nucleus. eLife *4*, e04659.

22. Castello, A., Fischer, B., Eichelbaum, K., Horos, R., Beckmann, B.M., Strein, C., Davey, N.E., Humphreys, D.T., Preiss, T., Steinmetz, L.M., et al. (2012). Insights into RNA biology from an atlas of mammalian mRNA-binding proteins. Cell *149*, 1393–1406.

23. Huang, R., Han, M., Meng, L., and Chen, X. (2018). Transcriptome-wide discovery of coding and noncoding RNA-binding proteins. Proc. Natl. Acad. Sci. USA *115*, E3879–E3887.

24. Bao, X., Guo, X., Yin, M., Tariq, M., Lai, Y., Kanwal, S., Zhou, J., Li, N., Lv, Y., Pulido-Quetglas, C., et al. (2018). Capturing the interactome of newly transcribed RNA. Nat. Methods *15*, 213–220.

25. Baltz, A.G., Munschauer, M., Schwanhäusser, B., Vasile, A., Murakawa, Y., Schueler, M., Youngs, N., Penfold-Brown, D., Drew, K., Milek, M., et al. (2012). The mRNA-bound proteome and its global occupancy profile on protein-coding transcripts. Mol. Cell *46*, 674–690.

26. He, C., Sidoli, S., Warneford-Thomson, R., Tatomer, D.C., Wilusz, J.E., Garcia, B.A., and Bonasio, R. (2016). High-resolution mapping of RNA-binding regions in the nuclear proteome of embryonic stem cells. Mol. Cell *64*, 416–430.

27. Queiroz, R.M.L., Smith, T., Villanueva, E., Marti-Solano, M., Monti, M., Pizzinga, M., Mirea, D.M., Ramakrishna, M., Harvey, R.F., Dezi, V., et al. (2019). Comprehensive identification of RNA–protein interactions in any organism using orthogonal organic phase separation (OOPS). Nat. Biotechnol. *37*, 169–178.

28. Gebauer, F., Schwarzl, T., Valcárcel, J., and Hentze, M.W. (2020). RNA-binding proteins in human genetic disease. Nat. Rev. Genet. *223*, 185–198.

29. Castello, A., Fischer, B., Frese, C.K., Curk, T., Krijgsveld, J., Hentze, M.W., Horos, R., Alleaume, A.-M., Foehr, S., and Hentze, M.W. (2016). Comprehensive identification of RNA-binding domains in human cells molecular cell resource comprehensive identification of RNA-binding domains in human cells. Mol. Cell *63*, 696–710.

30. Aktaş, T., Avşar Ilık, İ., Maticzka, D., Bhardwaj, V., Pessoa Rodrigues, C., Mittler, G., Manke, T., Backofen, R., and Akhtar, A. (2017). DHX9 suppresses RNA processing defects originating from the Alu invasion of the human genome. Nature *544*, 115–119.

31. Maticzka, D., Ilik, I.A., Aktas, T., Backofen, R., and Akhtar, A. (2018). uvCLAP is a fast and non-radioactive method to identify in vivo targets of RNA-binding proteins. Nat. Commun. *91*, 1142.

32. Singh, R., and Green, M.R. (1993). Sequence-specific binding of transfer RNA by glyceraldehyde-3-phosphate dehydrogenase. Science *259*, 365–368.

33. Palmer, L.E., Weiss, M.J., Paralkar, V.R., Trabucchi, M., Bottini, S., and Mukherjee, N. (2017). YODEL: Peak calling software for HITS-CLIP data. F1000Research *61138*, 1138.

34. Jaiswal, H., Conz, C., Otto, H., Wölfle, T., Fitzke, E., Mayer, M.P., and Rospert, S. (2011). The chaperone network connected to human ribosome-associated complex. Mol. Cell. Biol. *31*, 1160–1173.

35. Aprile-Garcia, F., Tomar, P., Hummel, B., Khavaran, A., and Sawarkar, R. (2019). Nascent-protein ubiquitination is required for heat shock–induced gene downregulation in human cells. Nat. Struct. Mol. Biol. *26*, 137–146.

36. Mann, H., Ben-Asouli, Y., Schein, A., Moussa, S., and Jarrous, N. (2003). Eukaryotic RNase P: role of RNA and protein subunits of a primordial catalytic ribonucleoprotein in RNA-based catalysis. Mol. Cell *12*, 925–935.

37. Williamson, D.S., Borgognoni, J., Clay, A., Daniels, Z., Dokurno, P., Drysdale, M.J., Foloppe, N., Francis, G.L., Graham, C.J., Howes, R., et al. (2009). Novel adenosine-derived inhibitors of 70 kDa heat shock protein, discovered through structure-based design. J. Med. Chem. *52*, 1510–1513.

38. Choquet, K., Forget, D., Meloche, E., Dicaire, M.J., Bernard, G., Vanderver, A., Schiffmann, R., Fabian, M.R., Teichmann, M., Coulombe, B., et al. (2019). Leukodystrophy-associated POLR3A mutations downregulate the RNA polymerase III transcript and important regulatory RNA BC200. J. Biol. Chem. *294*, 7445–7459.

39. Roberts, T.C., Hart, J.R., Kaikkonen, M.U., Weinberg, M.S., Vogt, P.K., and Morris, K.V. (2015). Quantification of nascent transcription by bromouridine immunocapture nuclear run-on RT-qPCR. Nat. Protoc. *10*, 1198–1211.

40. Sawarkar, R., and Paro, R. (2013). Hsp90@chromatin.nucleus: an emerging hub of a networker. Trends Cell Biol. *23*, 193–201.

41. Gerber, A., Ito, K., Chu, C.S., and Roeder, R.G. (2020). Gene-specific control of tRNA expression by RNA Polymerase II. Mol. Cell *78*, 765–778.

42. Wu, L., Pan, J., Thoroddsen, V., Wysong, D.R., Blackman, R.K., Bulawa, C.E., Gould, A.E., Ocain, T.D., Dick, L.R., Errada, P., et al. (2003). Novel small-molecule inhibitors of RNA polymerase III. Eukaryot. Cell *2*, 256–264.

43. Chen, L., Xu, W., Liu, K., Jiang, Z., Han, Y., Jin, H., Zhang, L., Shen, W., Jia, S., Sun, Q., et al. (2021). 5′ Half of specific tRNAs feeds back to promote corresponding tRNA gene transcription in vertebrate embryos. Sci. Adv. *7*, eabh0494.

44. Wang, Y., Tao, E.W., Tan, J., Gao, Q.Y., Chen, Y.X., and Fang, J.Y. (2023). tRNA modifications: insights into their role in human cancers. Trends Cell Biol. *33*, 1035–1048.

45. Baryshnikova, A., Costanzo, M., Myers, C.L., Andrews, B., and Boone, C. (2013). Genetic interaction networks: toward an understanding of heritability. Annu. Rev. Genomics Hum. Genet. *14*, 111–133.

46. Kato, M., Han, T.W., Xie, S., Shi, K., Du, X., Wu, L.C., Mirzaei, H., Goldsmith, E.J., Longgood, J., Pei, J., et al. (2012). Cell-free formation of RNA granules: low complexity sequence domains form dynamic fibers within hydrogels. Cell *149*, 753–767.

47. Ganassi, M., Mateju, D., Bigi, I., Mediani, L., Poser, I., Lee, H.O., Seguin, S.J., Morelli, F.F., Vinet, J., Leo, G., et al. (2016). A surveillance function of the HSPB8-BAG3-HSP70 chaperone complex ensures stress granule integrity and dynamism. Mol. Cell *63*, 796–810.

48. Yang, P., Mathieu, C., Kolaitis, R.M., Zhang, P., Messing, J., Yurtsever, U., Yang, Z., Wu, J., Li, Y., Pan, Q., et al. (2020). G3BP1 is a tunable switch that

triggers phase separation to assemble stress granules. Cell *181*, 325–345.e28.

49. Zhao, R., Kakihara, Y., Gribun, A., Huen, J., Yang, G., Khanna, M., Costanzo, M., Brost, R.L., Boone, C., Hughes, T.R., et al. (2008). Molecular chaperone Hsp90 stabilizes Pih1/Nop17 to maintain R2TP complex activity that regulates snoRNA accumulation. J. Cell Biol. *180*, 563–578.
50. Herold, N., Will, C.L., Wolf, E., Kastner, B., Urlaub, H., and Lührmann, R. (2009). Conservation of the protein composition and electron microscopy structure of *Drosophila melanogaster* and human spliceosomal complexes. Mol. Cell. Biol. *29*, 281–301.
51. Vogel, J.L., Parsell, D.A., and Lindquist, S. (1995). Heat-shock proteins Hsp104 and Hsp70 reactivate mRNA splicing after heat inactivation. Curr. Biol. *5*, 306–317.
52. Ros, M., Nguyen, A.T., Chia, J., Le Tran, S., Le Guezennec, X., McDowall, R., Vakhrushev, S., Clausen, H., Humphries, M.J., Saltel, F., et al. (2020). ER-resident oxidoreductases are glycosylated and trafficked to the cell surface to promote matrix degradation by tumour cells. Nat. Cell Biol. *22*, 1371–1381.
53. Gumiero, A., Conz, C., Gesé, G.V., Zhang, Y., Weyer, F.A., Lapouge, K., Kappes, J., Von Plehwe, U., Schermann, G., Fitzke, E., et al. (2016). Interaction of the cotranslational Hsp70 Ssb with ribosomal proteins and rRNA depends on its lid domain. Nat. Commun. *71*, 1–12.
54. Roehr, J.T., Dieterich, C., and Reinert, K. (2017). Flexbar 3.0 - SIMD and multicore parallelization. Bioinformatics *33*, 2941–2942.
55. Smith, T., Heger, A., and Sudbery, I. (2017). UMI-tools: modeling sequencing errors in Unique Molecular Identifiers to improve quantification accuracy. Genome Res. *27*, 491–499.
56. Heinz, S., Benner, C., Spann, N., Bertolino, E., Lin, Y.C., Laslo, P., Cheng, J.X., Murre, C., Singh, H., and Glass, C.K. (2010). Simple combinations of lineage-determining transcription factors prime cis-regulatory elements required for macrophage and B cell identities. Mol. Cell *38*, 576–589.
57. Ramírez, F., Ryan, D.P., Grüning, B., Bhardwaj, V., Kilpert, F., Richter, A.S., Heyne, S., Dündar, F., and Manke, T. (2016). deepTools2: a next generation web server for deep-sequencing data analysis. Nucleic Acids Res. *44*, W160–W165.
58. Dobin, A., Davis, C.A., Schlesinger, F., Drenkow, J., Zaleski, C., Jha, S., Batut, P., Chaisson, M., and Gingeras, T.R. (2013). STAR: ultrafast universal RNA-seq aligner. Bioinformatics *29*, 15–21.
59. Baer, M., Nilsen, T.W., Costigan, C., and Altman, S. (1990). Structure and transcription of a human gene for H1 RNA, the RNA component of human RNase P. Nucleic Acids Res. *18*, 97–103.
60. Girbig, M., Misiaszek, A.D., Vorländer, M.K., et al. (2021). Cryo-EM structures of human RNA polymerase III in its unbound and transcribing states. Nat. Struct. Mol. Biol. *28*, 210–219.

Please cite this article in press as: Leone et al., HSP70 binds to specific non-coding RNA and regulates human RNA polymerase III, Molecular Cell (2024), https://doi.org/10.1016/j.molcel.2024.01.001



## STAR★METHODS

### KEY RESOURCES TABLE

| REAGENT or RESOURCE | SOURCE | IDENTIFIER |
|---|---|---|
| Antibodies | | |
| Rabbit HSPA1A polyclonal antibody | R&D systems/ Biotechne | AF1663; RRID:AB_2233171 |
| Mouse anti-FLAG monoclonal antibody | Sigma-Aldrich | F3165-2MG; RRID:AB_259529 |
| Rabbit anti-POLR3A polyclonal antibody | Abcam | ab96328; RRID:AB_10678851 |
| Rabbit anti-Beta Tubulin polyclonal antibody | Cell signaling Technology | 2146; RRID:AB_2210545 |
| Mouse anti-HuR (3A2) monoclonal | Santa Cruz | sc-5261; RRID:AB_627770 |
| Rabbit anti-POP1 polyclonal | Proteintech | 12029-1-AP; RRID:AB_2166477 |
| Rabbit anti-RPP21 polyclonal | AssayGenie | CAB14424 |
| Chemicals, peptides, and recombinant proteins | | |
| Dulbecco's Modified Eagle's Medium - high glucose | Sigma-Aldrich | Cat# D5671 |
| Fetal Bovine Serum, Research Grade | Sigma-Aldrich | Cat# F0804 |
| L-glutamine solution | Sigma-Aldrich | Cat# G7513 |
| Penicillin-streptomycin solution | Sigma-Aldrich | Cat# P4333 |
| Zeocin | Invitrogen | Cat# R25001 |
| Blasticidin S | Carl Roth | Cat# CP14.1 |
| Hygromycin B | ThermoFisher Scientific | Cat# 10687010 |
| Tetracycline | Sigma-Aldrich | Cat# T7660 |
| Triton-X100 | Sigma-Aldrich | Cat# 93443 |
| Tween-20 | Sigma-Aldrich | Cat# P1379 |
| PBS | Gibco | Cat# 14190144 |
| IGEPAL® CA-630 | Sigma-Aldrich | Cat# I8896 |
| Sodium deoxycholate | Sigma-Aldrich | Cat# D6750 |
| Ethylenediaminetetraacetic acid | Sigma-Aldrich | Cat# 798681 |
| Sodium chloride | Sigma-Aldrich | Cat# S3014 |
| Tris-HCl | Invitrogen | Cat# 15568-025 |
| RNase I | Invitrogen | Cat# AM2294 |
| RNase A | Thermo Scientific | Cat# EN0531 |
| Magnesium chloride | Sigma-Aldrich | Cat# M8266 |
| 1x LDS buffer | Invitrogen | Cat# NP0007 |
| DTT | Merck | Cat# 3870 |
| Di(N-succinimidyl) glutarate | Sigma-Aldrich | Cat# 80424-50MG-F |
| T4 Polynucleotide Kinase | NEB | Cat# M0201S |
| 1% methanol-free formaldehyde | Thermo Scientific | Cat# 28906 |
| Glycine | Sigma-Aldrich | Cat# 1041691000 |
| PIPES | Sigma-Aldrich | Cat# 80635 |
| Potassium chloride | Sigma-Aldrich | Cat# 60128 |
| Sodium dodecyl sulfate | Sigma-Aldrich | Cat# L3771 |
| EGTA | Sigma-Aldrich | Cat# 324626 |
| N-Lauroylsarcosine sodium salt | Sigma-Aldrich | Cat# 61743 |
| Proteinase K | Sigma-Aldrich | Cat# P2308 |
| TURBO DNase | Thermo Scientific | Cat# AM2238 |
| 2-(N-morpholino)ethanesulfonic acid | Sigma-Aldrich | Cat# M3671 |
| RNase inhibitor | Thermo Scientific | Cat# AM2694 |

(*Continued on next page*)

Please cite this article in press as: Leone et al., HSP70 binds to specific non-coding RNA and regulates human RNA polymerase III, Molecular Cell (2024), https://doi.org/10.1016/j.molcel.2024.01.001





*Continued*

| REAGENT or RESOURCE | SOURCE | IDENTIFIER |
|---|---|---|
| T4 RNA Ligase 1 | NEB | Cat# M0204L |
| SuperScript III | Invitrogen | Cat# 18080093 |
| RNaseH | NEB | Cat# M0297S |
| CircLigase | Epicentre/Illumina | Cat# CL9021K |
| Hepes | Sigma-Aldrich | Cat# H4034 |
| Beta-mercaptoethanol | Sigma-Aldrich | Cat# M6250 |
| Protease inhibitor | Sigma-Aldrich | Cat# 1187358000 |
| VER155008 inhibitor | Sigma-Aldrich | Cat# SML0271 |
| Recombinant HSPA1A | Cayman Chemicals | Cat# 22739 |
| Recombinant GFP | Sino Biological | Cat# 13105-S07E |
| [alpha-$^{32}$P] CTP | Perkinelmer | Cat# BLU008X250UC |
| Phosphocreatine disodium salt hydrate | Sigma-Aldrich | Cat# P7936 |
| Pifithrin μ | Sigma-Aldrich | Cat# P0122 |
| Nucleotide triphosphate mix | Thermo Scientific | Cat# R0481 |
| DMSO | Sigma-Aldrich | Cat#276855 |
| Trizol reagent | Invitrogen | Cat#15596026 |
| 5-Bromouridine 5′-triphosphate sodium salt | Sigma-Aldrich | Cat# B7166 |
| Firefly luciferase RNA | Promega | Cat# L4561 |
| RNA Polymerase III Inhibitor - CAS 577784-91-9 - | Calbiochem | Cat# 557403 |
| Lipofectamine RNAiMax | Invitrogen | Cat# 13778075 |
| **Critical commercial assays** | | |
| NEBNext Ultra II DNA Library Prep kit | NEB | Cat# NEB E7645S |
| High Sensitivity DNA Chips | Agilent | Cat# 5067–4626 |
| Bioanalyzer 2100 | Agilent | Cat# G2939BA |
| BCA assay | Thermo Scientific | Cat# 23225 |
| Takara PrimeScript RT reaction kit | Takara | Cat# RR047A |
| Takara TB Green Premix Ex-Taq | Takara | Cat# RR420L |
| TruSeq stranded Total RNA | Illumina | Cat# 20020599 |
| **Deposited data** | | |
| Deep-sequencing data generated in this study | GEO database (https://www.ncbi.nlm.nih.gov/geo/) | GEO: GSE191245 |
| **Experimental models: cell lines** | | |
| HEK293 Flp-In T-Rex | Asifa Aktar, Freiburg | N/A |
| HEK293 Flp-In T-Rex PolR3C-3FHBH | Present study | N/A |
| HEK293 Flp-In T-Rex HSPA1A-3FHBH | Present study | N/A |
| HEK293 Flp-In T-Rex HSPA8-3FHBH | Present study | N/A |
| HEK293 Flp-In T-Rex GFP-3FHBH | Present study | N/A |
| HEK293 Flp-In T-Rex HSPA9-3FHBH | Present study | N/A |
| HEK293 Flp-In T-Rex HSP90AA1-3FHBH | Present study | N/A |
| HEK293 Flp-In T-Rex PPIA-3FHBH | Present study | N/A |
| HEK293 Flp-In T-Rex PPIL2-3FHBH | Present study | N/A |
| HEK293 Flp-In T-Rex HSPB1-3FHBH | Present study | N/A |
| HEK293 Flp-In T-Rex HSPB4-3FHBH | Present study | N/A |
| HEK293 Flp-In T-Rex HSPB5-3FHBH | Present study | N/A |
| HEK293 Flp-In T-Rex CCT5-3FHBH | Present study | N/A |
| HEK293 Flp-In T-Rex CCT8-3FHBH | Present study | N/A |
| HEK293 Flp-In T-Rex HNRNPC-3FHBH | Present study | N/A |
| HEK293 Flp-In T-Rex GAPDH-3FHBH | Present study | N/A |

(*Continued on next page*)

Please cite this article in press as: Leone et al., HSP70 binds to specific non-coding RNA and regulates human RNA polymerase III, Molecular Cell (2024), https://doi.org/10.1016/j.molcel.2024.01.001



*Continued*

| REAGENT or RESOURCE | SOURCE | IDENTIFIER |
|---|---|---|
| **Oligonucleotides** | | |
| Primers used for RT-PCR and RT-qPCR, and oligonucleotides for RNA interference, see Table S5 | Present study | N/A |
| **Recombinant DNA** | | |
| pcDNA5-GFP-3FHBH | Asifa Aktar, Freiburg | N/A |
| pcDNA5-hnRNPC-3FHBH | Asifa Aktar, Freiburg | N/A |
| DEST-B-3FHBH-pcDNA5-FRT-TO | Asifa Aktar, Freiburg | N/A |
| pOG44 | Renato Paro, Zurich, | N/A |
| pcDNA5-HSPA1A-3FHBH | Present study | N/A |
| pcDNA5-HSPA8-3FHBH | Present study | N/A |
| pcDNA5-HSPA9-3FHBH | Present study | N/A |
| pcDNA5-HSPA14-3FHBH | Present study | N/A |
| pcDNA5-HSP90AA1-3FHBH | Present study | N/A |
| pcDNA5-PPIA-3FHBH | Present study | N/A |
| pcDNA5-PPIL2-3FHBH | Present study | N/A |
| pcDNA5-HSPB1-3FHBH | Present study | N/A |
| pcDNA5-HSPB4-3FHBH | Present study | N/A |
| pcDNA5-HSPB5-3FHBH | Present study | N/A |
| pcDNA5-CCT5-3FHBH | Present study | N/A |
| pcDNA5-CCT8-3FHBH | Present study | N/A |
| pcDNA5-GAPDH-3FHBH | Present study | N/A |
| pcDNA5-RPP29-3FHBH | Present study | N/A |
| pcDNA5-POLR3C-3FHBH | Present study | N/A |
| pSupS1 (Ser pre-tRNA) | Nayef Jarrous, Jerusalem | N/A |
| pJA2 M1 RNA | Nayef Jarrous, Jerusalem | N/A |
| **Software and algorithms** | | |
| Flexbar, version 3.3 | https://github.com/seqan/flexbar/releases | Roehr et al.[54] |
| UMI Tools, version 0.5.1 | https://pubmed.ncbi.nlm.nih.gov/28100584/ | Smith et al.[55] |
| TrimGalore, version 0.4.4 | http://www.bioinformatics.babraham.ac.uk/projects/trim_galore/ | N/A |
| Bbmap, version 37.54 | https://jgi.doe.gov/data-and-tools/bbtools/bb-tools-user-guide/ | N/A |
| YODEL | N/A | Palmer et al.[33] |
| Homer annotatePeaks.pl | N/A | Heinz et al.[56] |
| Deeptools2 | N/A | Ramírez et al.[57] |
| **Other** | | |
| Bioruptor 300 | Diagenode | Cat# B01020001 |
| Dynabeads™ His-Tag Isolation | Invitrogen | Cat# 10103D |
| Dynabeads™ MyOne™ Streptavidin C1 | Invitrogen | Cat# 65001 |
| Covaris tubes | Covaris | Cat# 520130 |
| Covaris S220 | Covaris | Cat# 500217 |
| Protein G magnetic beads | Life Technologies | Cat# 10004D |
| DNA Clean and Concentrator | Zymo Research | Cat# D4033 |
| FLAG-coupled agarose beads | Millipore | Cat# A2220 |

Please cite this article in press as: Leone et al., HSP70 binds to specific non-coding RNA and regulates human RNA polymerase III, Molecular Cell (2024), https://doi.org/10.1016/j.molcel.2024.01.001



## RESOURCE AVAILABILITY

### Lead contact

Further information and requests for resources and reagents should be directed to and will be fulfilled by the lead contact, Ritwick Sawarkar (rs2099@cam.ac.uk)

### Materials availability

Reagents generated in this study are available upon request.

### Data and code availability

- All genomic datasets generated in this study have been deposited to GEO and are publicly available as of the date of publication. Accession numbers are listed in the key resources table.
- All custom scripts described herein are available on the Sawarkar Lab GitHub (https://github.com/). All original code has been deposited at Zenodo and is publicly available as of the date of publication. DOIs are listed in the key resources table.
- Any additional information required to reanalyze the data reported in this paper is available from the lead contact upon request.

## EXPERIMENTAL MODEL AND STUDY PARTICIPANT DETAILS

### Cell culture

HEK293 Flp-In T-Rex cells were cultured in DMEM high glucose medium supplemented with 10% FBS (Sigma-Aldrich F0804), 2mM L-glutamine (Sigma-Aldrich, G7513) and 1% penicillin-streptomycin (Sigma-Aldrich, P4333). Cells were kept at 37 °C in 5% $CO_2$ incubator. All cell lines were routinely checked for mycoplasma contamination by PCR.

## METHOD DETAILS

### Plasmid cloning

For generation of clones for human proteins, hORFs in pDONOR vector were purchased from BIOSS, University of Freiburg and cloned into pCDNA5-FRT/To vector with a C- term 3FHBH tag (kind gift from Ibrahim Avsar Ilik, Max Plank Institute, Freiburg) using Gateway LR clonase II enzyme kit (Life Technologies 11791020). pSupS1 and pJA2 M1 RNA were kindly provided by Prof. Nayef Jarrous (The Hebrew University of Jerusalem, Jerusalem)

### Plasmid transfection

HEK293 T-Rex Flp-In T-Rex cells were transfected using calcium phosphate protocol. To generate stable expression cell lines Flp-In T-Rex HEK293 were grown in 100 μg/ml zeocin (Invitrogen, R25001) for at least a week before transfection. Stable positive clones were selected for at least 2 weeks in 15 μg/ml blasticidin S (Carl Roth CP14.1) and 100 μg/ml hygromycin B (ThermoFisher Scientific, 10687010). Expression of chaperone protein was induced with 1 μg/ml tetracycline (Sigma-Aldrich, T7660).

### Tandem Affinity Purification

Cell were washed in 1xPBS and collected by scraping in NLB buffer (1xPBS; 300mM NaCl; 1% Triton-X100; 0.1% Tween-20). Cell lysis was obtained by pulsed ultrasonication (5 cycles, 30'' On, 30'' Off, at High intensity using Diagenode Bioruptor 300). Lysates were incubated 10 minutes at 4°C with Dynabeads™ His-Tag Isolation (Invitrogen, 10103D). After one wash with NLB buffer, proteins were eluted with 250mM imidazole in NLB buffer and incubated for 45 minutes rotating at 4°C with Dynabeads™ MyOne™ Streptavidin C1 (Invitrogen, 65001). After one wash in HSB buffer (50mM Tris-HCl, pH 7.4; 1M NaCl; 1% Igepal; 0.1% SDS; 0.5% Na-deoxycholate; 1mM EDTA) and one wash in NDB buffer (50mM Tris-HCl, pH 7.4; 100mM NaCl; 0.1% Tween-20). Beads containing purified proteins were resuspended in NDB buffer and used for PNK assay and FLASH-seq.

### Polynucleotide kinase (PNK) assay

Cells were grown as monolayers and irradiated on ice with 200mJ/$cm^2$ of 254nm UV light. After washing in 1xPBS, cells were collected by scraping in NLB buffer (1xPBS; 300mM NaCl; 1% Triton-X100; 0.1% Tween-20) and lysed by pulsed ultrasonication (5 cycles, 30'' On, 30'' Off, at High intensity using Diagenode Bioruptor 300). Cell lysates were subjected to tandem affinity purification as described above. To produce PNK accessible 5'-ends, "minus RNase" samples were incubated with 0.05U/μl of RNase I at 37°C for one minute. For a complete digestion of RNA "plus RNase" samples were treated with NDB buffer containing 2U/μl of RNase I (Invitrogen, AM2294) and 0.02μg/μl of RNase A (Thermo Scientific, EN0531) at 37 °C for 15 minutes. After RNase treatment, beads were washed once with HSB, once with NDB buffer and twice with PNK buffer (20mM Tris-HCl pH 7.4; 100mM MgCl2; 0.2% Tween-20). 1/10 of the affinity purified complexes were eluted for 10 minutes at 70°C in 1x LDS buffer (Invitrogen, NP0007) containing 25mM DTT and analysed by SDS PAGE and Western blot. The rest of the affinity purified complexes were radiolabelled with 0.1 μCi/μl γ-$^{32}$P ATP by T4 polynucleotide kinase (1U/μl) in PNK buffer for 30 minutes at 37 °C shaking at 1100rpm. Beads were washed twice with

PNK buffer and protein-RNA complexes were eluted for 10 minutes at 70°C in 1x LDS buffer (Invitrogen, NP0007) containing 25mM DTT. Samples were analysed by SDS PAGE and autoradiography.

### Chromatin immunoprecipitation and sequencing

Cells were fixed using 2mM Di(N-succinimidyl) glutarate (DSG; Sigma-Aldrich, 80424-50MG-F) for 40 minutes in 1xPBS at room temperature and 1% methanol-free formaldehyde (Thermo Scientific, 28906) was added in the last 10 minutes, followed by 5 min blocking in 0.125 M glycine. Cells were washed twice with ice-cold PBS. The cell pellet was resuspended in Farnham buffer (5 mM PIPES, pH 8; 85 mM KCl; 0.5% Igepal). Cell suspensions were sonicated for 3 minutes in 1 ml Covaris tubes (Covaris, 520130) using Covaris S220 with the following settings: peak power = 75; duty factor = 2; cycles/ burst = 200. Isolated nuclei were washed with Farnham buffer and suspended in shearing buffer (10 mM Tris-HCl, pH 8; 0.1% SDS; 1 mM EDTA). Chromatin was sheared by sonication in 1-ml Covaris tubes using the following settings: peak power = 140; duty factor = 5; cycles/burst = 200, time = 25–30 min. Debris were removed by centrifugation at 16000 x g. A DNA fragment–size distribution of 200–600 bp was considered as ideal chromatin for ChIP. Chromatin was diluted 1:1 with IP buffer (10 mM Tris-HCl, pH 8; 100 mM NaCl, 1 mM EDTA, 0.5 mM EGTA, 0.1% sodium deoxycholate, 0.1% N-lauroylsarcosine) to achieve a final 0.05% SDS concentration. Good quality chromatin (200 μg) was used for immunoprecipitation. Protein G magnetic beads (Life Technologies, 10004D) were incubated (rotated) with 5–10 μ g of FLAG antibody (Sigma-Aldrich, F1804-200UG) for 6 hours at 4 °C. This bead–antibody complex was then incubated overnight at 4 °C with sheared chromatin. An aliquot of chromatin was saved as input DNA. Beads were washed and DNA–protein complexes were eluted from the beads by heating at 65 °C in elution buffer (50 mM Tris-HCl, pH 8.0, 10 mM EDTA and 1% SDS). Crosslinking was reversed for 6 h at 70 °C and samples were treated with 200 μg/ml RNase A (Thermo Scientific, EN0531) and 200 μg/ml proteinaseK (Sigma-Aldrich, P2308). ChIP DNA was purified with phenol–chloroform extraction and ethanol precipitation. Some 2–5 ng of immunoprecipitated DNA was used for library preparation for next-generation sequencing. Sequencing libraries were prepared using the NEBNext Ultra II DNA Library Prep kit for Illumina (NEB E7645S). Library size distribution was monitored by capillary electrophoresis (Agilent 2100 Bioanalyzer, High Sensitivity DNA Chips (Agilent, 5067–4626)). Libraries were sequenced paired end on NextSeq500 or NovaSeq6000 instruments (Illumina).

### FLASH sequencing

FLASH-seq protocol was applied as described in Aktaş et al.[30] and Maticzka et al.[31] Briefly, doxycycline-induced HEK293 T-Rex Flp-In T-Rex cells were rinsed in 1xPBS and crosslinked with 0.2mJ/cm2 UV-C irradiation. Crosslinked cells were collected by scraping and pelleted by centrifugation. Cells were resuspended in NLB buffer and lysed and by water bath-sonication. Target protein of interest were affinity purified in tandem with nickel-charged paramagnetic beads and streptavidin-coupled paramagnetic beads against the tagged protein of interest as described above (Tandem affinity purification). To trim the crosslinked RNA, the beads were resuspended with 1 mL of NDB (50 mM Tris- Cl, pH 7.4; 100 mM NaCl, 0.1% Tween-20), to which 2 μL of TURBO DNase (AM2238, Thermo Fisher Scientific) and 10 μL of diluted RNaseI (1:2000–1:8000 dilution in NDB from 100 U/μL stock (AM2294, Thermo Fisher Scientific)) were added. The solution was incubated at 37 °C for 3 min and immediately transferred on ice. Dephosphorylation of cyclic phosphate groups was carried out with T4 PNK (10 U/μL, M0201, NEB) in a low pH buffer (25 mM MES (2-(N-morpholino)ethanesulfonic acid), pH 6.0; 50 mM NaCl; 10mM MgCl2; 0.1% Tween-20; 20U RNasin (Thermo fisher, AM2694); 10 U PNK; 20 min at 37 °C). Custom-made, barcoded 3'-adapters were ligated using T4 RNA Ligase 1, for 1 hr at 25°C. Custom FLASH adapters contained two barcodes and random nucleotides adjacent to the 3'-adapters according to the pattern NNBBNTTTTTTNN (N: random tag nucleotide, T: tag nucleotide, B: RY-space tag nucleotide). Random tags were used to merge PCR-duplicates, regular tags were used to specify the pulldown condition, and semi-random RY-space tags were used to distinguish the biological replicates (RR: replicate A, YY: replicate B, R: purine, Y: pyrimidine). Excess adapters were washed away, and RNA was isolated with Proteinase K treatment and column purification (Zymo DNA Clean and Concentrator). Isolated RNA was reverse transcribed with SuperScript III (Invitrogen, 18080093) and treated with RNaseH (M0297S NEB). cDNA was column-purified and circularized with CircLigase (Epicentre/Illumina, CL9021K) for 16hrs. Circularized cDNA was directly PCR amplified, quantified with Qubit/Bioanalyzer and sequenced on Illumina NextSeq 500 or NextSeq 3000 in paired-end mode.

### Bioinformatic analysis

FLASH-seq data were demultiplexed using Flexbar, version 3.3.[54] For each sample, UMIs were extracted using UMITools, version 0.5.1[55] followed by adapter removal with TrimGalore, version 0.4.4 [http://www.bioinformatics.babraham.ac.uk/projects/trim_galore/]. Potential readthroughs into the barcode and UMI region were removed by clipping the last 13 bases from the 3' ends of first mate reads. Paired-end reads were merged using bbmerge from bbmap, version 37.54 [https://jgi.doe.gov/data-and-tools/bbtools/bb-tools-user-guide/]. The demultiplexed and processed reads were mapped to the human genome build hg38 using STAR, version 2.6.0b[58] with the addition of the parameters ''–outFilterMultimapNmax 150 –outFilterScoreMinOverLread 0 –outFilterMatchNminOverLread 0 –outFilterMatchNmin 0 –alignEndsType EndToEnd –alignIntronMax 100000''. UMITools, version 0.5.1[55] was used to combine duplicated reads into individual crosslinking events. For each FLASH sample, enriched regions were identified using YODEL.[33] Resulting peak regions were annotated using homer annotatePeaks.pl.[56] Bigwig files were generated using deeptools2.[57] Yodel peaks were cleared from alternative chromosomes.

Please cite this article in press as: Leone et al., HSP70 binds to specific non-coding RNA and regulates human RNA polymerase III, Molecular Cell (2024), https://doi.org/10.1016/j.molcel.2024.01.001





### Whole cell extract preparation

Cells were harvested by scraping in ice-cold 1xPBS and washed once in Buffer A (10 mM KCl, 1.5 mM MgCl2, 0.5 mM DTT, 10 mM Hepes, pH 7.9). Cells were resuspended in one packed cell volume of Buffer A, incubated on ice for 10 minutes and passed through a 19G needle 10 times. After adjusting the salt concentration to 200mM KCl the cells were passed through a 21G needle. Cell lysis was obtained by pulsed ultrasonication (10 cycles, 30'' On, 30'' Off, at High intensity using Diagenode Bioruptor 300), complete lysis was monitored by phase contrast microscopy. Cellular debris were pelleted at 20000 x g for 20 minutes at 4°C. The supernatant was used for immunoprecipitation or for *in vitro* transcription experiments.

### Immunoprecipitation

Whole cell extracts were prepared as described above. Immunoprecipitation was carried out using FLAG-coupled agarose beads (Millipore, A2220) in IP buffer (20mM Tris-HCl pH 7.5; 100mM KCl; 0.5mM DTT; 0.2mM EDTA; 20% glycerol). Protein content was measured by BCA assay (Thermo Scientific 23225). 250-500μg of protein extracts were incubated rotating at 4°C for 16 hours with 20-40 μl of IP buffer pre-washed FLAG-coupled agarose beads. After incubation, beads were washed three times with TNET-150 buffer (20mM Tris-HCl pH7.5; 150 mM NaCl; 0.1 mM EDTA; 1mM beta-mercaptoethanol; 0.01% v/v Triton-X100) and three times with PA buffer (50mM Tris-HCl pH7.5; 0.1M $NH_4Cl$; 10mM $MgCl_2$). Immunoprecipitated proteins were eluted in 20-40μl of 1x TNET and 1x PA buffer containing 300ng/μl of FLAG peptide for 10 minutes at room temperature. Eluted proteins were used in the RNase P assay or Western blot.

### RNase P assay

RNase P assay was performed as described in Mann et al.[36] Briefly, 5μl of the 3FHBH-RPP29 co-immunoprecipitated RNaseP holoenzyme or the M1 RNA control were incubated in 20μl 1xTNET 1xPA buffer supplemented with 1mM DTT, 1X Protease inhibitor (Sigma-Aldrich, 1187358000) and 10U of RNase inhibitor (Ambion, AM2694) at 37°C for 1 hour. Reactions were supplemented either with 20μM VER155008 HSP70 inhibitor (Sigma-Aldrich, SML0271-5MG), 50nM recombinant HSPA1A (Cayman Chemicals, 22739) or 50nM recombinant GFP (Sino Biological, 13105-S07E). The yeast pre-tRNASer (pSupS1), was transcribed *in vitro* by T7 RNA polymerase in the presence of [alpha-$^{32}$P] CTP, purified on a 7M urea 5% polyacrylamide gel, and was used at a final concentration of 500 nM (ca. 2,000 cpm per reaction). Gels were exposed to phosphorimager screen at -20°C for 16 hours.

### In vitro transcription

In vitro transcription assays were performed using whole cell extracts or RNA Pol III holoenzyme co-purified with 3FHBH-PolR3C tandem affinity purification. IVT reaction were carried as described in Baer et al.[59] Briefly, 25 μl of whole cell extracts or 20 μl of RNA Pol III-containing streptavidin paramagnetic beads were incubated in a final volume of 50μl for 30-60 minutes in 1X transcription buffer (12 mM Tris-HCl pH7.9; 5 mM $MgCl_2$; 80 mM KCl, 0.5 mM DTT; 20 mM creatine phosphate; 0.5 mM each of ATP, UTP, CTP, GTP; 20U of RNase inhibitor) containing 500 ng of pUC-tRNA-Tyr reporter plasmid. Reactions were supplemented either with 20 μM Pifithrin μ HSP70 inhibitor (Sigma-Aldrich P0122-5MG), 140 μM DMSO (Sigma-Aldrich, 276855), 50 nM recombinant HSPA1A (Cayman Chemicals, 22739) or 50 nM recombinant GFP (Sino Biological, 13105-S07E). IVT reaction were terminated by adding 10 volumes of Trizol reagent (Invitrogen, 15596026).

### Nuclear Run-on

Nuclear Run-on assays were performed as described in Roberts et al.[39] Briefly, nuclei were obtained from cells incubated in NP-40 lysis buffer (10 mM Tris-HCl, pH 7.4, 10 mM NaCl, 3 mM MgCl2 and 0.5% (vol/vol) NP-40). Run-on was carried out incubating nuclei in transcription buffer (10 mM Tris-HCl, pH 8.3, 2.5 mM MgCl2, 150 mM KCl, 2 mM DTT, 1mM each of ATP, CTP, GTP; 0.5 mM of each UTP and Bromo-UTP; 20U of RNase inhibitor). Run-on reactions were carried out in the presence of 20μM VER155008 HSP70 inhibitor (Sigma-Aldrich, SML0271-5MG) or 140 μM DMSO (Sigma-Aldrich, 276855) and incubated at 30 °C for 40 minutes. Reactions were stopped with 10 volumes of Trizol reagent (Invitrogen, 15596026) containing 0.01pg/μl of bromouridine-labelled *in vitro* transcribed renilla luciferase used as positive spike-in control, or 0.01 pg/μl firefly luciferase (Promega, L4561) used as negative spike-in control.

### RNA purification and reverse transcription

RNA purification was performed using Trizol reagent (Invitrogen, 15596026) according to the manufacturer instructions. RT reaction was done using Takara PrimeScript RT reaction kit (RR047A) and qPCRs were done using Takara TB Green Premix Ex-Taq (RR420L) according to the manufacturer instructions.

### RNA interference

HEK293 Flp-In T-Rex cells were plated 24 hours prior siRNA transfection. HSPA1A/B and HSPA8 specific siRNA were ordered from Microsynth as set of three different siRNA duplexes (Table S5). The three siRNA for each target pooled to a final stock concentration of 10 mM each. siRNAs were transfected using Lipofectamine RNAiMax according to the manufacturer's instructions (Invitrogen, 13778075). siRNAs were transfected at 20 nM. Cells were further incubated for 48 h before being harvested for analysis. Knockdown efficiency was confirmed by RT-qPCR.

Please cite this article in press as: Leone et al., HSP70 binds to specific non-coding RNA and regulates human RNA polymerase III, Molecular Cell (2024), https://doi.org/10.1016/j.molcel.2024.01.001



### RNA sequencing

RNA purification was performed using Trizol reagent (Invitrogen, 15596026) according to the manufacturer instructions. TruSeq stranded Total RNA (Gold), Illumina was used for the construction of sequencing libraries.

### Electrophoretic mobility shift assay (EMSA)

T7 transcribed RNA was heat denatured at 65 °C for 5 minutes and flash-cooled on ice. Recombinant HSPA1A was incubated with RNA in 1X binding buffer (20 mM Tris–HCl, 100mM NaCl, 1mM EDTA, 1mM DTT, 0.02% Tween-20, pH 7.0) for 1 hr at 25 °C. Samples were resuspended in 10% glycerol just before loading on a 3% agarose gel. SYBR gold-stained agarose gels were used to detect the mobility pattern of RNA.

### TGCA analysis

Raw read counts from TCGA RNA-seq data were downloaded from source (https://portal.gdc.cancer.gov/repository), and cancer types with more than 5 normal tissue controls were used for subsequent analyses. 15 cancer types from 378 patients were kept after filtering. A "median score" of (medianPT-medianNT)/(medianPT+medianNT) was calculated from the raw counts-per-million (where PT stands for Primary Tumour and NT for Normal Tissue), and the pairwise Pearson correlation between the cancer expression of the whole proteome and that of HSPA8/HSPA1B was computed. The observations were then fitted to a normal distribution and six members of the RNA Pol III complex were found to be among the top 10% of correlators. The probability of randomly extracting a protein with correlation greater or equal to these was thus calculated as the complement of their cumulative probability distribution:

$$P(coef. > x) = 1 - \int_{-inf}^{-x} p.d.f.(x)dx$$

Where x is the Pearson coefficient of the protein considered and p.d.f. stands for probability distribution function. The probability of independently extracting N proteins belonging to the same complex was then simply computed as the product of the individual probabilities:

$$P_{tot} = \prod_{i=1}^{6} P_i$$

A map of all 17 subunits comprising RNA Pol III was generated using BioRender (BioRender.com) utilising cryo-EM maps from Girbig et al.[60]

TCGA cancer types analysed: BLCA (bladder urothelial carcinoma), BRCA (breast invasive carcinoma), COAD (Colon adenocarcinoma), HNSC (head and neck squamous cell carcinoma), KICH (kidney chromophobe), KIRC (kidney renal clear cell carcinoma), KIRP (kidney renal papillary cell carcinoma), LIHC (liver hepatocellular carcinoma), LUAD (lung adenocarcinoma), LUSC (lung squamous cell carcinoma), PRAD (prostate adenocarcinoma), READ (Rectum adenocarcinoma), STAD (stomach adenocarcinoma), THCA (thyroid carcinoma), UCEC (uterine corpus endometrial carcinoma).